Regularity and a priori error analysis on anisotropic meshes of a Dirichlet problem in polyhedral domains

Hengguang Li, Serge Nicaise

Regularity and a priori error analysis on anisotropic meshes of a Dirichlet problem in polyhedral domains

Hengguang Li* and Serge Nicaise†

Abstract

Consider the Poisson equation on a polyhedral domain with the given data in a weighted L^2 space. We establish new regularity results for the solution with possible vertex and edge singularities and propose anisotropic finite element algorithms approximating the singular solution in the optimal convergence rate. In particular, our numerical method involves anisotropic graded meshes with less geometric constraints but lacking the maximum angle condition. Optimal convergence on such meshes usually requires smoother given data. Thus, a by-product of our result is to extend the application of these anisotropic meshes to broader practical computations by allowing almost-L^2 data. Numerical tests validate the theoretical analysis.

1 Introduction

We consider the standard Dirichlet problem associated with the Laplace operator in a bounded polyhedral domain $\Omega \subset \mathbb{R}^3$:

$$\begin{cases} -\Delta u = f & \text{in } \Omega, \\ u = 0 & \text{on } \partial\Omega. \end{cases} \tag{1}$$

The solution of equation (1) is uniquely defined in $H_0^1(\Omega)$ for $f \in H^{-1}(\Omega)$ [17, 24]. The solution regularity, however, is determined by both the smoothness of the given function and the geometry of the domain. In particular, the solution may possess singularities in high-order Sobolev spaces near the non-smooth boundary points even when f is smooth [15, 18, 20, 21]. These singularities, often being the main theoretical concern, can also severely deteriorate the efficacy of the numerical approximation.

For a three-dimensional polyhedral domain, given a sufficiently smooth function f, there are two types of singularities in the solution associated with the non-smooth boundary points: the vertex singularity and the anisotropic edge singularity. In order to improve the convergence of the finite element approximation, one has to take both singularities into account. Consequently, *anisotropic* graded meshes are usually expected on such domains. This is different from the *isotropic* graded meshes on two-dimensional polygonal domains, where only corner (vertex) singularities need special numerical treatment.

The development of optimal finite element methods (FEMs) for equation (1) has been a technically challenging task, due to the combination of different types of singularities and due to the

*Department of Mathematics, Wayne State University, Detroit, MI 48202, USA, li@wayne.edu

†Université de Valenciennes et du Hainaut Cambrésis, LAMAV, FR CNRS 2956, Institut des Sciences et Techniques of Valenciennes, F-59313 - Valenciennes Cedex 9 France, Serge.Nicaise@univ-valenciennes.fr

complexity in the three-dimensional geometry. The existing anisotropic methods [1, 4, 6, 8, 9, 25] converge to the singular solution in the optimal rate but usually require confining angle conditions for the simplex or restrictive conditions for the domain. Recently, a new anisotropic FEM has been formulated [23] based on recursive mesh refinements. With less geometric requirements on the simplex and on the domain, this algorithm leads to conforming triangulations that however violates the maximum angle condition in simplexes [7, 22]. Based on the regularity estimates in anisotropic weighted spaces $M^m_{\boldsymbol{\beta}}(\Omega)$ [10] and the interpolation error analysis in $M^m_{\boldsymbol{\beta}}(\Omega)$, this algorithm yields optimal FEMs approximating the singular solution of equation (1). The tradeoff for such flexibility on mesh generation is that the result in [23], even for the lowest-order case, requires that f at least belongs to $M^2_{\boldsymbol{\beta}}(\Omega) \subset H^2_{loc}(\Omega)$. This is mainly due to the fact that unlike the usual full-regularity results, the regularity estimate in $M^m_{\boldsymbol{\beta}}(\Omega)$ has no "shifting" in space indices; while when f merely belongs to $L^2(\Omega)$, the solution does not have extra regularity in the edge direction to compensate for the lack of mesh shape regularity. It is apparent that this smoothness requirement on the given data can be an undesired constraint limiting the anisotropic algorithm in practical computations.

In this paper, we alleviate the regularity constraint on the given data by developing new anisotropic finite element algorithms for equation (1) when f possesses less regularity than $H^2_{loc}(\Omega)$. In particular, we introduce a weighted L^2 space ($L^2_{\boldsymbol{\mu}^*}(\Omega)$ in Definition 9) consisting of functions with mild smoothness assumptions near the edges. With $f \in L^2_{\boldsymbol{\mu}^*}(\Omega)$, through a series of estimates regarding different directional derivatives of the solution, we establish new anisotropic regularity results for equation (1), which we formulate in Corollaries 3.5 and 3.7. Besides their applications in numerical methods, these results themselves can be of theoretical interest. Then, we propose an optimal finite element algorithm (Algorithm 4.4). Its validation is based on interpolation error analysis in anisotropic weighted spaces. This method is different from those in [23], because for $f \in L^2_{\boldsymbol{\mu}^*}(\Omega)$, the solution is no longer in $M^2_{\boldsymbol{\beta}}(\Omega)$, and therefore the algorithm and error analysis in the aforementioned paper do not apply.

The paper is organized as follows. In Section 2, we introduce necessary notation and existing results regarding the finite element approximation of equation (1). We also define the weighted L^2 space for the given function. In Section 3, we establish anisotropic regularity estimates provided that $f \in L^2_{\boldsymbol{\mu}^*}(\Omega)$. In Section 4, we first review the anisotropic mesh developed in [23]. Then we propose the anisotropic FEM for equation (1) with less-regular given data. In Section 5, we include detailed interpolation error analysis for the anisotropic finite element algorithm in weighted spaces. These optimal interpolation error estimates in turn lead to the conclusion that the proposed FEMs obtain the optimal convergence rate approximating the target problem. Numerical tests are implemented on two typical polyhedral domains (the prism and the Fichera corner) and the results are reported in Section 6. These numerical results are in agreement with our theoretical prediction and hence validate our method. The Appendix (Section 7) contains further remarks for some arguments in previous sections.

Throughout the text below, we adopt the bold notation for vector fields. Let T be a triangle (resp. tetrahedron) with vertices a, b, c (resp. a, b, c, d). Then, we denote T by its vertices: $\triangle^3 abc$ for the triangle and $\triangle^4 abcd$ for the tetrahedron, where the sup-index implies the number of vertices for T. We denote by ab the open line segment with endpoints a and b and denote by $\overrightarrow{ab}$ the vector from a to b. By $a \sim b$ (resp. $a \lesssim b$), we mean that there exists a constant $C > 0$ independent of a and b, such that $C^{-1}a \le b \le Ca$ (resp. $a \le Cb$). The generic constant $C > 0$ in our estimates may be different at different occurrences. It will depend on the computational domain, but not on the functions involved or the mesh level in the finite element algorithms. In addition, both of the terms are used to represent the same directional derivative: $\partial_1 = \partial_x$, $\partial_2 = \partial_y$, and $\partial_3 = \partial_z$.

2 Preliminaries

In this section, we introduce the notation and recall some existing results regarding the solution of equation (1).

2.1 The finite element approximation

By a polyhedral domain $\Omega \subset \mathbb{R}^3$, we mean a bounded domain with a Lipschitz boundary $\partial\Omega$ made of plane faces (i.e., its boundary is a finite union of polygons). Thus, the boundary of Ω is smooth, except at the vertex points and along the edges. In a neighborhood of a vertex c, Ω coincides with a three-dimensional cone, while near an interior point of an edge e, Ω resembles a dihedral angle.

For a bounded domain $\mathcal{O}$ of $\mathbb{R}^3$, let $H^m(\mathcal{O})$, $m \geq 0$, be the usual Sobolev space that consists of functions defined in $\mathcal{O}$ whose kth derivatives are square-integrable in $\mathcal{O}$ for $0 \leq k \leq m$ (hence $L^2(\mathcal{O}) := H^0(\mathcal{O})$). Let $H^m_{loc}(\Omega) := \{v,\ v \in H^m(G)$, for any open subset G with compact closure $\bar{G} \subset \Omega\}$. The trace operator from $H^1(\Omega)$ into $H^{\frac{1}{2}}(\partial\Omega)$ will be denoted by γ. We denote by

$$H^1_0(\Omega) = \{u \in H^1(\Omega),\ \gamma u = 0 \text{ on } \partial\Omega\},$$

which is clearly a closed subspace of $H^1(\Omega)$. Then, for $f \in L^2(\Omega)$, the variational solution $u \in H^1_0(\Omega)$ of problem (1) is defined by

$$a(u,v) := \int_\Omega \nabla u \cdot \nabla v \, dx = (f,v) := \int_\Omega f v \, dx, \qquad \forall v \in H^1_0(\Omega). \tag{2}$$

Let $\mathcal{T}_n$ be a triangulation of Ω with tetrahedra. Let $S_n \subset H^1_0(\Omega)$ be the linear Lagrange finite element space associated with $\mathcal{T}_n$. Then, the finite element solution $u_n \in S_n$ for equation (1) is given by

$$a(u_n, v_n) = (f, v_n), \quad \forall v_n \in S_n. \tag{3}$$

Remark 2.1 *By Poincaré's inequality, the bilinear form $a(\cdot,\cdot)$ is both continuous and coercive on $H^1_0(\Omega)$. Then, by Céa's Lemma [12, 13], u_n is the best approximation from S_n in $H^1_0(\Omega)$*

$$|u - u_n|_{H^1(\Omega)} \leq \inf_{v_n \in S_n} |u - v_n|_{H^1(\Omega)}. \tag{4}$$

It is well known that the solution u may not belong to $H^2(\Omega)$ due to the presence of the non-smooth points (vertices and edges) on the boundary. On a standard quasi-uniform triangulation $\mathcal{T}_n$, the limited regularity of u in the Sobolev space can result in a sub-optimal convergence rate for the finite element approximation. Namely,

$$\|u - u_n\|_{H^1(\Omega)} \leq C h^s \|u\|_{H^{s+1}(\Omega)}, \tag{5}$$

where h is the mesh size in $\mathcal{T}_n$ and $0 < s < 1$ depends on the geometry of the domain.

For equation (1), there are two types of singularities in the solution that may affect the convergence of numerical methods. The vertex singularity appears in the neighborhood of a vertex and concentrates at the vertex. The edge singularity occurs in the neighborhood of an edge; it is however anisotropic in the sense that the solution is smoother in the direction along the edge than toward the edge. Consequently, anisotropic graded meshes are frequently applied to improve the convergence of the finite element solution.

Due to the complexity in the three-dimensional mesh refinements, existing mesh grading algorithms on polyhedral domains usually require restrictive geometric conditions on the mesh and on the domain. For example, the meshes in [2, 16] are based on the method of dyadic partitioning. These meshes are isotropic and optimal only for weaker singular solutions. The meshes in [1, 3, 4, 5] are based on a coordinate transformation from a quasi-uniform mesh. They are anisotropic near the edges and require confining angle conditions for the simplex. For these meshes, quasi-optimal convergence rate is obtained in [4], while optimal convergence rate is hinted in [3, 5]. The meshes in [8, 9] are also anisotropic and lead to optimal convergence rate. The algorithm, however, requires extra steps for prism refinements to maintain the angle condition in the simplex. There are also tensor-product anisotropic meshes based on 2D graded meshes [6, 25] that are usually effective on a domain with simple geometry.

A new anisotropic mesh refinement algorithm has been recently proposed in [23] for the finite element approximation of singular solutions. Based on recursive decompositions of tetrahedra, the new algorithm is simple, explicit, and distinguishable from other existing three-dimensional mesh algorithms by requiring less geometric conditions on the simplexes and on the domain. However, due to the lack of mesh shape regularity and due to the anisotropic nature of the singularity, in order for the associated FEMs in [23] to obtain the optimal convergence rate for equation (1), the given function f is expected to belong to a subspace of $H^2_{loc}(\Omega)$. For less-regular given data, which occurs often in practical computations, the study of such anisotropic FEMs for singular solutions remains an open investigation.

In this paper, we fill the gap by studying the finite element approximation of equation (1) with less-regular given data. In particular, we shall show that for $f \in L^2_{loc}(\Omega)$, some additional smoothness in f near the edges is sufficient to compensate for the lack of shape regularity in the mesh. Therefore it is possible to develop optimal finite element algorithms on the anisotropic meshes for the singular solution. In what follows, before we present the anisotropic finite element scheme, we first define a proper weighted L^2 space for the given data.

2.2 The domain and the given data

We denote by $\mathcal{E}$ the finite set of edges and by $\mathcal{C}$ the finite set of vertices of Ω. We also denote by $\mathcal{E}_c \subset \mathcal{E}$ the set of edges joining at $c \in \mathcal{C}$ and by $\mathcal{C}_e \subset \mathcal{C}$ the set of endpoints of $e \in \mathcal{E}$. In addition, if e is an edge with an opening angle $\omega_e > \pi$, it is called *singular*, otherwise it is called *regular*. Denote by Γ_c the cone that coincides with the domain Ω at $c \in \mathcal{C}$. Let ν_c be the first positive eigenvalue of the Laplace-Beltrami operator (with Dirichlet boundary conditions) on the intersection of Γ_c with the unit sphere. Then, if $-\frac{1}{2} + (\nu_c + 1/4)^{1/2} < \frac{1}{2}$, c is called *singular*. For $e \in \mathcal{E}$ and $c \in \mathcal{C}$, we set

$$\begin{cases} \lambda_e = \frac{\pi}{\omega_e} \text{ if } e \text{ is singular, } \lambda_e = \infty \text{ otherwise;} \\ \lambda_c = -1/2 + (\nu_c + 1/4)^{1/2} \text{ if } c \text{ is singular, } \lambda_c = \infty \text{ otherwise.} \end{cases} \tag{6}$$

To better describe the singular behavior of the solution near the non-smooth points, we further define the distance functions. For any $c \in \mathcal{C}$ (resp. $e \in \mathcal{E}$), we define $R_c(x)$ (resp. $r_e(x)$) to be the distance from $x \in \Omega$ to c (resp. to e). We further define $\theta_{c,e}(x) := \frac{r_e(x)}{R_c(x)}$ as the angular distance from x to the edge of e near c. Then, for any vertex $c \in \mathcal{C}$ and edge $e \in \mathcal{E}$, as in [10], we define the following subsets of Ω

$$\begin{cases} \mathcal{V}_c = \{x \in \Omega,\ R_c(x) < \varepsilon\}, \\ \mathcal{V}_c^e = \{x \in \mathcal{V}_c,\ \theta_{c,e}(x) < \varepsilon\}, \\ \mathcal{V}_c^0 = \{x \in \mathcal{V}_c,\ \theta_{c,e}(x) \geq \varepsilon,\ \forall e \in \mathcal{E}_c\}, \\ \mathcal{V}_e^0 = \{x \in \Omega,\ R_c(x) \geq \varepsilon,\ \theta_{c,e}(x) < \varepsilon,\ \forall c \in \mathcal{C}_e\}, \end{cases} \tag{7}$$

with $\varepsilon > 0$ small enough, such that all these sets are disjoint for different vertices c and edges e. We further define

$$\mathcal{V}^0 = \Omega \setminus \left((\cup_{c\in\mathcal{C}} \mathcal{V}_c) \cup (\cup_{e\in\mathcal{E}} \mathcal{V}_e^0) \right). \tag{8}$$

It is clear that the subsets in (7) are neighborhoods of different non-smoothness points on the boundary. In the neighborhoods $\mathcal{V}_e^0$ and $\mathcal{V}_c^e$, we choose a local Cartesian coordinate system in which the edge $e \in \mathcal{E}$ lies on the z-axis. Let $\alpha_\perp = (\alpha_1, \alpha_2)$ consist of the first two entries of the multi-index $\alpha = (\alpha_1, \alpha_2, \alpha_3) \in \mathbb{Z}^3_{\geq 0}$. Therefore, in $\mathcal{V}_e^0$ and $\mathcal{V}_c^e$, $\partial^{\alpha_\perp} = \partial_x^{\alpha_1}\partial_y^{\alpha_2}$ is a partial derivative in a direction perpendicular to the edge e.

Then, we define the following weighted space.

Definition 2.2 *(The Weighted L^2 Space) For $\boldsymbol{\mu} = (\mu_e)_{e\in\mathcal{E}}$ with $\mu_e \in \mathbb{R}$, we introduce the function:*

$$w_{\boldsymbol{\mu}}(x) = \begin{cases} 1 & \text{if } x \in \mathcal{V}^0 \bigcup \left(\bigcup_{c\in\mathcal{C}} \mathcal{V}_c^0 \right), \\ \theta_{c,e}^{-\mu_e} & \text{if } x \in \mathcal{V}_c^e, \quad \forall c \in \mathcal{C}, e \in \mathcal{E}_c, \\ r_e^{-\mu_e} & \text{if } x \in \mathcal{V}_e^0, \quad \forall e \in \mathcal{E}. \end{cases} \tag{9}$$

For any $G \subseteq \Omega$, define the space

$$L^2_{\boldsymbol{\mu}}(G) = \{v \in L^2_{\mathrm{loc}}(\Omega),\ w_{\boldsymbol{\mu}} v \in L^2(G)\}.$$

This space is a Hilbert space with its natural inner product

$$(v, g)_{\boldsymbol{\mu}} = \int_\Omega w_{\boldsymbol{\mu}}(x)^2 v(x) g(x)\, dx, \quad \forall v, g \in L^2_{\boldsymbol{\mu}}(\Omega),$$

and associated norm $\|v\|_{\boldsymbol{\mu}} = (v, v)_{\boldsymbol{\mu}}^{\frac{1}{2}}$, for $v \in L^2_{\boldsymbol{\mu}}(\Omega)$.

Remark 2.3 *Note that for $\mu_e \geq 0$, $L^2_{\boldsymbol{\mu}}(\Omega) \subseteq L^2(\Omega)$ and in order to be in the space $L^2_{\boldsymbol{\mu}}$, an L^2 function needs additional smoothness in the direction perpendicular to the edge. In the next section, we explore the anisotropic structure of the singular solution in equation (1). In particular, we derive regularity estimates for each directional derivative of the solution when the given function belongs to the proper weighted L^2 space. Note that when f is only in $L^2(\Omega)$, the second derivative of u in the edge direction does not possess extra regularity (see [4, 10, 9]). This extra regularity in the edge direction, available when $f \in M^2_{\boldsymbol{\beta}}(\Omega) \subset H^2_{loc}(\Omega)$ [10], plays an important role in validating the anisotropic mesh that violates the maximum angle condition. Our regularity estimates shall show that with some mild restriction on the weight $w_{\boldsymbol{\mu}}$, for $f \in L^2_{\boldsymbol{\mu}}(\Omega)$, extra regularity of the solution in the edge direction, to a certain degree, becomes feasible. We will then use these results to develop optimal FEMs for singular solutions by allowing the given data in a less-regular weighted L^2 space. In addition, our regularity analysis themselves can be of theoretical interest for some readers.*

Throughout the paper, we fix the parameter $\boldsymbol{\mu^*} = (\mu_e^*)_{e\in\mathcal{E}}$, such that

$$\mu_e^* \in [1/2, \lambda_e) \quad \text{if } \omega_e > \pi; \qquad \text{and} \qquad \mu_e^* = 0 \quad \text{otherwise.} \tag{10}$$

Note that based on (6), $\lambda_e > 1/2$. Thus, the parameter μ_e^* is well defined. Then, we study equation (1) with $f \in L^2_{\boldsymbol{\mu^*}}(\Omega)$.

3 Regularity analysis

In this section, we obtain anisotropic regularity results for equation (1) with $f \in L^2_{\boldsymbol{\mu}^*}(\Omega)$. Our analysis is based on regularity estimates in different sub-regions (see (7)) of the domain near the vertices and edges. To better understand the dependence of the solution on the domain and on the given data, we begin with a slightly different assumption on f: we assume $f \in L^2_{\boldsymbol{\mu}}(\Omega)$, where $\boldsymbol{\mu} = (\mu_e)_{e\in\mathcal{E}}$ satisfies

$$\mu_e \in (0, \lambda_e) \quad \text{if } \omega_e > \pi; \qquad \text{and} \qquad \mu_e = 0 \quad \text{otherwise.} \tag{11}$$

It is clear that $L^2_{\boldsymbol{\mu}^*}(\Omega) \subseteq L^2_{\boldsymbol{\mu}}(\Omega) \subset L^2(\Omega)$ if $\mu_e \leq \mu_e^*$, for all $e \in \mathcal{E}$. Therefore, the regularity results obtained for $f \in L^2_{\boldsymbol{\mu}}(\Omega)$ still hold for $f \in L^2_{\boldsymbol{\mu}^*}(\Omega)$, but it will simplify the exposition.

3.1 Regularity estimates in $\mathcal{V}_e^0$

Let us start with an improved regularity of the solution along the edges for $f \in L^2_{\boldsymbol{\mu}}(\Omega)$.

Theorem 3.1 *Let $u \in H^1_0(\Omega)$ be the solution of (2) with $f \in L^2_{\boldsymbol{\mu}}(\Omega)$ as defined in (11). Then for any $e \in \mathcal{E}$, we have*

$$u \in L^2_{\boldsymbol{\mu}}(\mathcal{V}_e^0), \qquad \nabla u \in L^2_{\boldsymbol{\mu}}(\mathcal{V}_e^0)^3, \tag{12}$$

$$\partial_3^2 u \in L^2_{\boldsymbol{\mu}}(\mathcal{V}_e^0), \tag{13}$$

where ∂_3 is the derivative in the direction of the edge e.

Proof. For a regular edge e, namely for which $\omega_e < \pi$, the results are immediate since we know that u belongs to $H^2(\mathcal{V}_e^0)$ (see [15] or [4, Theorem 2.4]). Hence it remains to prove the results for a singular edge e for which $\omega_e > \pi$.

Let ξ be a fixed interior point of a singular edge e and let η be a cut-off function such that $\eta \equiv 1$ in a neighborhood of ξ and $\eta \equiv 0$ in a neighborhood of the vertices and the other edges. Take the z-axis parallel to the edge e. Without loss of generality, we can assume that ξ is at the origin and we drop the index e. Denote by $D = \Sigma \times \mathbb{R}$ the dihedral truncated cone that coincides with Ω near ξ, where Σ is the truncated two-dimensional cone of opening ω, namely

$$\Sigma = \{(r\cos\theta, r\sin\theta) \in \mathbb{R}^2 : 0 < r < 1, 0 < \theta < \omega\}.$$

Since the property (13) is only of interest along the edge, we can assume that the support of η is included in D.

Now $\tilde{u} := \eta u$ is clearly a weak solution of

$$-\Delta\tilde{u} = \tilde{f} \text{ in } D, \tag{14}$$

where $\tilde{f}$ is given by

$$\tilde{f} = \eta f - 2\nabla u \cdot \nabla\eta - u\Delta\eta \in L^2(D).$$

To have the regularity $\tilde{u} \in L^2_{\boldsymbol{\mu}}(D) = \{v \in L^2(D),\ r^{-\mu}v \in L^2(D)\}$ (where r is the distance to the edge $\{0\} \times \mathbb{R}$ of D), we use Theorem 2.4 of [4] that shows that

$$r^{\delta-2}\tilde{\eta}u \in L^2(\Omega) \quad \text{and} \quad r^{\delta-1}\nabla(\tilde{\eta}u) \in L^2(\Omega)^3, \tag{15}$$

for any $\delta > 1 - \lambda_e$, where $\tilde{\eta}$ is similar to η, except that $\tilde{\eta} \equiv 1$ on the support of η. This result directly leads to (12) and in particular to $\tilde{u} \in L^2_{\boldsymbol{\mu}}(D)$.

At this stage we apply a Fourier transform technique (see for instance [19]), namely performing a partial Fourier transform in z, we see that $V = \mathfrak{F}_z(\tilde{u})(\xi)$ is solution of

$$\left\{ \begin{array}{cc} -\Delta V + \xi^2 V = \mathfrak{F}_z(\tilde{f})(\xi), & \text{in} \quad \Sigma, \\ V = 0, & \text{on} \quad \partial\Sigma. \end{array} \right. \tag{16}$$

By Parseval's identity, we have

$$\|\tilde{f}\|^2_{L^2_{\boldsymbol{\mu}}(D)} = \int_{\mathbb{R}} \|\mathfrak{F}_z(\tilde{f})(\xi)\|^2_{L^2_{\boldsymbol{\mu}}(\Sigma)}\, d\xi,$$

where

$$\|v\|^2_{L^2_{\boldsymbol{\mu}}(\Sigma)} = \int_{\Sigma} |r(x)^{-\mu} v(x)|^2\, dx.$$

Then, we apply Corollary 2.12 of [11] that furnishes

$$\xi^2 \|V\|^2_{L^2_{\boldsymbol{\mu}}(\Sigma)} \lesssim \|\mathfrak{F}_z(\tilde{f})(\xi)\|^2_{L^2_{\boldsymbol{\mu}}(\Sigma)}.$$

Taking the square of this estimate, using the Fourier transform back and again Parseval's identity, we find that

$$\|\partial_3^2 \tilde{u}\|^2_{L^2_{\boldsymbol{\mu}}(D)} \lesssim \|\tilde{f}\|^2_{L^2_{\boldsymbol{\mu}}(D)}. \tag{17}$$

This proves (13). ■

3.2 Regularity estimates in $\mathcal{V}^e_c$

Now we describe the extra regularity in a neighborhood of a vertex $c \in \mathcal{C}$ that is an endpoint of the singular edge e. Recall that Γ_c is the cone that coincides with Ω at c and R_c is the distance to c. Then, for any $\beta \in \mathbb{R}$, $k \in \mathbb{Z}_{\geq 0}$, we define the space

$$V^k_\beta(\Gamma_c) = \{v \in L^2_{\mathrm{loc}}(\Gamma_c),\ R_c^{\beta+|\alpha|-k} D^\alpha v \in L^2(\Gamma_c),\ \forall |\alpha| \leq k\}.$$

We fix a cut-off function χ such that $\chi \equiv 1$ in a neighborhood of c and $\chi \equiv 0$ in a neighborhood of the other vertices of Ω. Note that the vertex singular exponent of problem (2) near c [18, 4] is given by

$$\lambda_{c,k} = -\frac{1}{2} \pm \sqrt{\nu_{c,k} + \frac{1}{4}},$$

where $\{\nu_{c,k}\}_{k=1}^\infty$ is the spectrum (repeated according to their multiplicity) of the positive Laplace-Beltrami operator L_G^{Dir} with Dirichlet boundary condition on the intersection G between Γ_c and the unit sphere. The associated singular function $\sigma_{c,k}$ is given by

$$\sigma_{c,k} = R_c^{\lambda_{c,k}} \varphi_{c,k},$$

where $\varphi_{c,k}$ is the eigenvector of L_G^{Dir} associated with $\nu_{c,k}$, namely

$$L_G^{\mathrm{Dir}} \varphi_{c,k} = \nu_{c,k} \varphi_{c,k}.$$

Then, we first have the regularity estimate for the regular part of the solution near the vertex.

Lemma 3.2 *Assume $\lambda_{c,k} \neq \frac{1}{2}$ for all $k \in \mathbb{N}$. Recall the cut-off function χ defined above. Let $u \in H^1_0(\Omega)$ be the solution of equation (2) with $f \in L^2_{\boldsymbol{\mu}}(\Omega)$ as defined in (11). Then χu admits the splitting*

$$\chi u = u_0 + \sum_{0<\lambda_{c,k}<\frac{1}{2}} c_k \sigma_{c,k}, \tag{18}$$

where $u_0 \in V^1_{-1}(\Gamma_c)$, $c_k \in \mathbb{C}$ and $\Delta u_0 \in L^2_{\boldsymbol{\mu}}(\Gamma_c)$. Furthermore we have

$$R_c^{-2} w_{\boldsymbol{\mu}} u_0 \in L^2(\Gamma_c) \text{ and } R_c^{-1} w_{\boldsymbol{\mu}} \nabla u_0 \in L^2(\Gamma_c)^3, \tag{19}$$

where $w_{\boldsymbol{\mu}}$ is defined as in (9):

$$w_{\boldsymbol{\mu}}(x) = \begin{cases} \theta_{c,e}^{-\mu_e} & \text{if } \theta_{c,e}(x) < \varepsilon, \ \forall e \in \mathcal{E}_c, \\ 1 & \text{else.} \end{cases}$$

Proof. We first apply Theorem 2.6 of [4] (see also Lemma 17.4 of [15]) that yields the decomposition (18) with $c_k \in \mathbb{C}$ and $u_0 \in V^1_{-1}(\Gamma_c)$ that can be split up in the form

$$u_0 = u_r + u_{\text{edge}},$$

with $u_r \in V^2_0(\Gamma_c) \cap H^1_0(\Gamma_c)$ and $u_{\text{edge}} \in V^1_{-1}(\Gamma_c)$. Note that $\sigma_{c,k}$ are harmonic function. Thus

$$\Delta u_0 = \Delta(\chi u)$$

and therefore Δu_0 belongs to $L^2_{\boldsymbol{\mu}}(\Gamma_c)$ owing to (12).

Note that $u_r \in V^2_0(\Gamma_c)$ and $u_{\text{edge}} \in V^1_{-1}(\Gamma_c)$ yields (19) far from the edges. Hence we only need to show extra regularities along the edge. Now, we fix one edge $e \in \mathcal{E}_c$. Without loss of generality we can assume that the edge e is contained in the z-axis and that c is at the origin. Fix further spherical coordinates (R, θ, φ) such that $\theta = 0$ corresponds to the z-axis (hence $R = R_c$ near c and $\theta = \theta_{c,e}$ near e).

To prove the extra regularity of u_0 along e, we notice that Theorem 2.7 of [4] shows that

$$R^{-1} \theta^{\delta_e - 1} \nabla u_{\text{edge}} \in L^2(\Gamma_c^e)^3,$$

for any $\delta_e \geq 0$ such that $\delta_e > 1 - \lambda_e$ if $\omega_e > \pi$, and $\delta_e = 0$ else, where

$$\Gamma_c^e = \{x \in \Gamma_c, \ \theta_{c,e} < \varepsilon\}.$$

As $\mu_e < \lambda_e$, we can always pick up δ_e, such that $1 - \mu_e \geq \delta_e > 1 - \lambda_e$ and therefore

$$R^{-1} \theta^{-\mu_e} \nabla u_{\text{edge}} \in L^2(\Gamma_c^e)^3. \tag{20}$$

For simplicity, let us write μ instead of μ_e.

Now we take advantage of the fact that $u_{\text{edge}}(0) = 0$ to write

$$u_{\text{edge}}(R, \theta, \varphi) = \int_0^R \frac{\partial u_{\text{edge}}}{\partial R}(s, \theta, \varphi)\, ds.$$

Hence using the Hardy operator H defined in [18, p. 28], we have

$$R^{-1} u_{\text{edge}}(R, \theta, \varphi) = H\left(\frac{\partial u_{\text{edge}}}{\partial R}(\cdot, \theta, \varphi)\right).$$

Since for almost all (θ, φ), we have

$$\int_0^\infty |\frac{\partial u_{\text{edge}}}{\partial R}(\cdot, \theta, \varphi)|^2 \, dR < \infty,$$

we can apply Hardy's inequality (see [18, p. 28]) to get

$$\int_0^\infty |R^{-1} u_{\text{edge}}(R, \theta, \varphi)|^2 \, dR \lesssim \int_0^\infty |\frac{\partial u_{\text{edge}}}{\partial R}(R, \theta, \varphi)|^2 \, dR.$$

Multiplying this estimate by $\theta^{-2\mu} \sin \varphi$ and integrating in θ and φ, we find that

$$\int_{\Gamma_c} |R^{-2} \theta^{-\mu} u_{\text{edge}}(x)|^2 \, dx \lesssim \int_{\Gamma_c} |R^{-1} \theta^{-\mu} \frac{\partial u_{\text{edge}}}{\partial R}(x)|^2 \, dx < \infty.$$

This shows that

$$R^{-2} \theta^{-\mu} u_{\text{edge}} \in L^2(\Gamma_c), \tag{21}$$

and yields the requested regularity of u_{edge} near the edge.

For the regular part u_r, in view of its regularity $V_0^2(\Gamma_c)$, we only need to show extra regularity along the edge e. Therefore we fix a cut-off function η depending only on θ that is equal to 1 in a neighborhood of $\theta = 0$, and equal to 0 outside a larger neighborhood of $\theta = 0$. Then the regularity $u_r \in V_0^2(\Gamma_c)$ implies that

$$R^{-1} \partial_j (\eta u_r) \in L^2(\Gamma_c), \quad \forall j = 1, 2, 3. \tag{22}$$

Now for $j \in \{1, 2, 3\}$, we write

$$\partial_j (\eta u_r)(R, \theta, \varphi) = -\int_\theta^\infty \frac{\partial}{\partial \theta} \partial_j (\eta u_r)(R, \tilde{\theta}, \varphi) \, d\tilde{\theta}.$$

Hence using the Hardy operator L defined in [18, p. 28], we have

$$\theta^{-1} \partial_j (\eta u_r)(R, \theta, \varphi)) = -L \left(\frac{\partial}{\partial \theta} \partial_j (\eta u_r)(R, \cdot, \varphi) \right).$$

Since for almost all (R, φ),

$$\int_0^\infty |\frac{\partial}{\partial \theta} \partial_j (\eta u_r)(R, \tilde{\theta}, \varphi)|^2 \tilde{\theta}^{1+2\epsilon} \, d\tilde{\theta} < \infty,$$

for all $\epsilon > 0$, we can apply Hardy's inequality (see [18, p. 28]) to get

$$\int_0^\infty |\tilde{\theta}^{\epsilon-1} \partial_j (\eta u_r)(R, \tilde{\theta}, \varphi)|^2 \tilde{\theta} \, d\tilde{\theta} \lesssim \int_0^\infty |\tilde{\theta}^\epsilon \frac{\partial \partial_j (\eta u_r)}{\partial \theta}(R, \tilde{\theta}, \varphi)|^2 \tilde{\theta} \, d\tilde{\theta},$$

for all $\epsilon > 0$. Integrating in R and φ, we find that for all $\epsilon > 0$,

$$\int_{\Gamma_c} |R^{-1} \theta^{\epsilon-1} \partial_j (\eta u_r)(x)|^2 \, dx \lesssim \int_{\Gamma_c} |R^{-1} \frac{\partial}{\partial \theta} \partial_j (\eta u_r)(x)|^2 \, dx < \infty.$$

By choosing ϵ small enough, we will have $\theta^{-\mu} \lesssim \theta^{\epsilon-1}$, and therefore we deduce that

$$R^{-1}\theta^{-\mu}\partial_j(\eta u_r) \in L^2(\Gamma_c), \quad \forall j = 1,2,3. \tag{23}$$

Now we take advantage of the fact that $u_r(0) = 0$ to write

$$\eta u_r(R,\theta,\varphi) = \int_0^R \frac{\partial(\eta u_r)}{\partial R}(s,\theta,\varphi)\, ds,$$

and with the help of Hardy's inequality and (23), we deduce that

$$R^{-2}\theta^{-\mu}\eta u_r \in L^2(\Gamma_c). \tag{24}$$

The conclusion (19) follows from (20), (21) (23), and (24). ■

Besides the estimates for low-order derivatives of u_0 in Lemma 3.2, we now derive the regularity estimate for the second derivative of u_0 along the edge.

Lemma 3.3 *Under the assumption of Lemma 3.2, let $u \in H_0^1(\Omega)$ be the solution of equation (2) with $f \in L^2_{\boldsymbol{\mu}}(\Omega)$ as defined in (11). Then u_0 from (18) satisfies*

$$\theta_{c,e}^{-\mu_e}\partial_3^2 u_0 \in L^2(\mathcal{V}_c^e), \quad \forall c \in \mathcal{C}, e \in \mathcal{E}_c, \tag{25}$$

where ∂_3 is the derivative in the direction of the edge e.

Proof. We assume that the edge e is contained in the z-axis and that c is at the origin. Fix the spherical coordinates (R,θ,φ), such that $\theta = 0$ corresponds to the z-axis (hence $R = R_c$ near c and $\theta = \theta_{c,e}$ near e). To simplify the notation, we shall drop the index e in μ_e. We use a dyadic covering technique. Namely, for all $j \in \mathbb{N}$, we define

$$\Sigma_{0j} := \{x \in \Gamma_c : 1 < 2^j|x| < 2\} \quad \text{and} \quad \Sigma_{1j} := \{x \in \Gamma_c : 1/2 < 2^j|x| < 4\},$$

which are respectively homothetic to

$$\hat{\Sigma}_0 := \{x \in \Gamma_c : 1 < |x| < 2\} \quad \text{and} \quad \hat{\Sigma}_1 := \{x \in \Gamma_c : 1/2 < |x| < 4\},$$

via the mapping

$$h_j : \Gamma_c \to \Gamma_c : x \to 2^j x.$$

For a fixed $j \in \mathbb{N}$, let us now set $\hat{u}_0(\hat{x}) = u_0(h_j^{-1}\hat{x})$. We fix a cut-off function $\hat{\eta}$ equal to 1 on $\hat{\Sigma}_0$ and equal to 0 outside $\hat{\Sigma}_1$. Then, applying the estimate (17) to $\hat{\eta}\hat{u}_0$, we find that

$$\|\theta(\hat{x})^{-\mu}\partial_3^2\hat{u}_0\|^2_{\hat{\Sigma}_{0,e}} \lesssim \|\theta(\hat{x})^{-\mu}\Delta\hat{u}_0\|^2_{\hat{\Sigma}_{1,e}} + \|\theta(\hat{x})^{-\mu}\nabla\hat{u}_0\|^2_{\hat{\Sigma}_{1,e}} + \|\theta(\hat{x})^{-\mu}\hat{u}_0\|^2_{\hat{\Sigma}_{1,e}},$$

where

$$\hat{\Sigma}_{0,e} = \{\hat{x} \in \hat{\Sigma}_0 : \theta(\hat{x}) < \varepsilon\} \quad \text{and} \quad \hat{\Sigma}_{1,e} = \{\hat{x} \in \hat{\Sigma}_1 : \theta(\hat{x}) < 2\varepsilon\}.$$

As $\hat{R}$ is equivalent to 1 on $\hat{\Sigma}_1$, this estimate implies that

$$\|\theta(\hat{x})^{-\mu}\partial_3^2\hat{u}_0\|^2_{\hat{\Sigma}_{0,e}} \lesssim \|\theta(\hat{x})^{-\mu}\Delta\hat{u}_0\|^2_{\hat{\Sigma}_{1,e}} + \|\hat{R}^{-1}\theta(\hat{x})^{-\mu}\nabla\hat{u}_0\|^2_{\hat{\Sigma}_{1,e}} + \|\hat{R}^{-2}\theta(\hat{x})^{-\mu}\hat{u}_0\|^2_{\hat{\Sigma}_{1,e}}.$$

Coming back to u_0 via the transformation h_j, we find

$$\|\theta(x)^{-\mu}\partial_3^2 u_0\|^2_{\Sigma_{0j,e}} \lesssim \|\theta(x)^{-\mu}\Delta u_0\|^2_{\Sigma_{1j,e}} + \|R^{-1}\theta(x)^{-\mu}\nabla u_0\|^2_{\Sigma_{1j,e}} + \|R^{-2}\theta(x)^{-\mu}u_0\|^2_{\Sigma_{1j,e}},$$

where

$$\Sigma_{0j,e} = \{x \in \Sigma_{0j},\ \theta(x) < \varepsilon\} \quad \text{and} \quad \Sigma_{1j,e} = \{x \in \Sigma_{1j},\ \theta(x) < 2\varepsilon\}.$$

Summing on $j \in \mathbb{N}$ and taking into account Lemma 3.2, we arrive at the estimate (25). ■

Recall λ_c in (6). Then, we have the weighted regularity estimate for the second derivative of the solution along the edge direction in the neighborhood of the vertex.

Theorem 3.4 *Under the assumption of Lemma 3.2, let $u \in H^1_0(\Omega)$ be the solution of equation (2) with $f \in L^2_{\boldsymbol{\mu}}(\Omega)$ as defined in (11). Then u satisfies*

$$R_c^{\beta_c}\theta_{c,e}^{-\mu_e}\partial_3^2 u \in L^2(\mathcal{V}_c^e), \quad \forall c \in \mathcal{C}, e \in \mathcal{E}_c, \tag{26}$$

where ∂_3 is the derivative in the direction of the edge e; and $\beta_c > \frac{1}{2} - \lambda_c$ if c is singular, $\beta_c = 0$ otherwise.

Proof. In view of the splitting (18), it suffices to show that each term satisfies the desired regularity estimate. Since $R_c^{\beta_c} \lesssim 1$, by Lemma 3.3, u_0 clearly satisfies

$$R_c^{\beta_c}\theta_{c,e}^{-\mu_e}\partial_3^2 u_0 \in L^2(\mathcal{V}_c^e).$$

The singular part (that is zero if c is not singular) satisfies it since by using spherical coordinates we see that $\partial_3^2\sigma_{c,k}$ behaves like $R_c^{\lambda_{c,k}-2}\theta_{c,e}^{\lambda_e}$. Hence direct calculations yield

$$R_c^{\beta_c}\theta_{c,e}^{-\mu_e}\partial_3^2\sigma_{c,k} \in L^2(\mathcal{V}_c^e),$$

for any $\beta_c > \frac{1}{2} - \lambda_c$. ■

Now, we extend our analysis and derive regularity estimates for derivatives of the solution both along and perpendicular to the edge direction.

Corollary 3.5 *Recall λ_e and λ_c in (6). Under the assumption of Lemma 3.2, let $u \in H^1_0(\Omega)$ be the solution of equation (2) with $f \in L^2_{\boldsymbol{\mu}}(\Omega)$ as defined in (11). For any $c \in \mathcal{C}$ and $e \in \mathcal{E}_c$, let $\gamma_c, \gamma_e \in [0,1]$ be such that $\gamma_c < \lambda_c + 1/2$ and $\gamma_e < \lambda_e$. Then, the following norms/seminorms of u are bounded by $\|f\|_{L^2_{\boldsymbol{\mu}}(\Omega)}$:*

$$\|R_c^{-1-\gamma_c}\theta_{c,e}^{-1-\gamma_e}u\|_{L^2(\mathcal{V}_c^e)}, \tag{27}$$

$$\|R_c^{-\gamma_c}\theta_{c,e}^{-\gamma_e}\partial_\perp u\|_{L^2(\mathcal{V}_c^e)}, \tag{28}$$

$$\|R_c^{-\gamma_c}\theta_{c,e}^{-1}\partial_3 u\|_{L^2(\mathcal{V}_c^e)}, \tag{29}$$

$$\|R_c^{1-\gamma_c}\theta_{c,e}^{1-\gamma_e}\partial_\perp^2 u\|_{L^2(\mathcal{V}_c^e)}, \tag{30}$$

$$\|R_c^{1-\gamma_c}\partial_\perp\partial_3 u\|_{L^2(\mathcal{V}_c^e)}, \tag{31}$$

$$\|R_c^{1-\gamma_c}\theta_{c,e}^{-\mu_e}\partial_3^2 u\|_{L^2(\mathcal{V}_c^e)}, \tag{32}$$

where ∂_3 is the derivative in the direction of e and $\partial_\perp$ is either ∂_1 or ∂_2.

Proof. Since we are interested in the regularity of u in $\mathcal{V}_c^e$, for a fixed vertex c and edge $e \in \mathcal{E}_c$, we use $R = R_c$ and $\theta = \theta_{c,e}$.

With the notation from [10], $f \in L^2_{\boldsymbol{\mu}}(\Omega)$ belongs to $M^0_{1-\boldsymbol{\beta}}(\Omega)$ with $\beta_{c'} = \gamma_{c'}$ and $\beta_{e'} = \gamma_{e'}$ for all vertices c' and edges e' (as $\gamma_{c'}\, \gamma_{e'} \in [0,1]$). Therefore, by Theorem 3.3 in [10], we have

$$R_c^{-1-\gamma_c} \theta_{c,e}^{-1-\gamma_e} u \in L^2(\mathcal{V}_c^e).$$

Therefore, (27) is proved.

Note $f \in L^2_{\boldsymbol{\mu}}(\Omega) \subset L^2(\Omega)$. According to Theorem 2.10 in [4], $u = u_r + u_s$ with $u_r \in H^2(\Omega) \cap H^1_0(\Omega)$ and u_s satisfying

$$R^{\beta-1}\theta^{\delta-1}\partial_\perp u_s \in L^2(\mathcal{V}_c^e), \quad R^{\beta-1}\theta^{-1}\partial_3 u_s \in L^2(\mathcal{V}_c^e),$$

where

$$\beta, \delta \geq 0, \quad \beta > 1/2 - \lambda_c, \quad \delta > 1 - \lambda_e. \tag{33}$$

Note $\beta - 1 \geq -1$ and $\beta - 1 > -1/2 - \lambda_c$; and $\delta - 1 \geq -1$ and $\delta - 1 > -\lambda_e$. Then, for the chosen γ_c and γ_e, we have

$$R^{-\gamma_c}\theta^{-\gamma_e}\partial_\perp u_s \in L^2(\mathcal{V}_c^e), \qquad R^{-\gamma_c}\theta^{-1}\partial_3 u_s \in L^2(\mathcal{V}_c^e). \tag{34}$$

To get (28) and (29), it then remains to prove a similar property for u_r. This is proved with the help of Hardy's inequalities (see [18, p. 28]). First by Lemma 7.1.1 of [21] (based on Hardy's inequalities), we have

$$R^{-1}\partial_j u_r \in L^2(\Omega), \quad \forall j = 1,2,3. \tag{35}$$

Now we fix any $j \in \{1,2,3\}$ and we again use the spherical coordinates (R, θ, φ) such that R is the distance to c and $\theta = 0$ corresponds to the edge e. By fixing a cut-off function $\eta_e \in \mathcal{D}(\mathbb{R})$ such that $\eta_e = 1$ in a neighborhood of 0, we can write for almost all R and φ

$$\eta_e(\theta')\partial_3 u_r(R,\theta',\varphi) = \int_0^{\theta'} \frac{\partial}{\partial\theta}\Big(\eta_e(\theta)\partial_j u_r(R,\theta,\varphi)\Big)\, d\theta,$$

since $\eta_e(\theta = 0)\partial_j u_r(R, \theta = 0, \varphi) = 0$ (because $u_r = 0$ on the boundary). This identity can be written as

$$R^{-1}\theta'^{-1}\eta_e(\theta')\partial_j u_r(R,\theta',\varphi) = H\left(R^{-1}\frac{\partial}{\partial\theta}\Big(\eta_e(\theta)\partial_j u_r(R,\theta,\varphi)\Big)\right)(\theta'),$$

where the operator H is defined by

$$(Hv)(t) = \frac{1}{t}\int_0^t v(s)\, ds.$$

Now we show that

$$R^{-1}\frac{\partial}{\partial\theta}\Big(\eta_e(\theta)\partial_j u_r(R,\theta,\varphi)\Big) \in L^2(\mathbb{R}), \text{ for almost all } R \in (0,R_0), \varphi \in (0,\pi), \tag{36}$$

for some $R_0 > 0$. Indeed by Leibniz's rule one has

$$R^{-1}\frac{\partial}{\partial\theta}\Big(\eta_e(\theta)\partial_j u_r(R,\theta,\varphi)\Big) = R^{-1}\eta_e'(\theta)\partial_j u_r + R^{-1}\frac{\partial}{\partial\theta}\partial_j u_r.$$

Hence by the regularity $u_r \in H^2(\Omega)$ and (35), we obtain

$$R^{-1}\frac{\partial}{\partial\theta}\Big(\eta_e(\theta)\partial_j u_r(R,\theta,\varphi)\Big) \in L^2(\Omega).$$

Since in spherical coordinates the Lebesgue measure is $R^2\sin\varphi dRd\theta d\varphi$, we get (36). This regularity allows us to apply Hardy's inequality and find that for almost all $R \in (0,R_0)$ and $\varphi \in (0,\pi)$,

$$\int_0^\infty |R^{-1}\theta'^{-1}\eta_e(\theta')\partial_j u_r(R,\theta',\varphi)|^2\,d\theta' \le 4\int_0^\infty |R^{-1}\frac{\partial}{\partial\theta}\Big(\eta_e(\theta)\partial_j u_r(R,\theta,\varphi)\Big)|^2\,d\theta.$$

Multiplying this estimate by $R^2\sin\varphi$ and integrating in $R \in (0,R_0)$ and $\varphi \in (0,\pi)$, we deduce that

$$\begin{aligned}\int_0^{R_0}\int_0^\infty\int_0^\pi |R^{-1}\theta'^{-1}\eta_e(\theta')\partial_j u_r(R,\theta',\varphi)|^2\,R^2\sin\varphi\,dRd\theta'd\varphi\\ \le 4\int_\Omega |R^{-1}\frac{\partial}{\partial\theta}\Big(\eta_e(\theta)\partial_j u_r(R,\theta,\varphi)\Big)|^2\,dx.\end{aligned}$$

This shows that

$$R^{-1}\theta^{-1}\partial_j u_r \in L^2(\mathcal{V}_e^c),$$

and with (34), we deduce that (28) and (29) hold.

Meanwhile, recalling that $u = u_r + u_s$, again by Theorem 2.10 in [4] and by (26), we get

$$R^\beta\theta^\delta\partial_\perp^2 u_s \in L^2(\mathcal{V}_e^c), \quad R^\beta\partial_\perp\partial_3 u_s \in L^2(\mathcal{V}_e^c) \quad R^\beta\theta^{-\mu_e}\partial_3^2 u \in L^2(\mathcal{V}_e^c), \tag{37}$$

where β and δ are defined in (33). By its definition, $1-\gamma_c \ge 0$, $1-\gamma_c > 1/2-\lambda_c$, and $1-\gamma_e \ge 0, 1-\gamma_e > 1-\lambda_e$. Therefore, since $u_r \in H^2(\Omega)$, (37) gives rise to

$$\begin{aligned}R^{1-\gamma_c}\theta^{1-\gamma_e}\partial_\perp^2 u = R^{1-\gamma_c}\theta^{1-\gamma_e}\partial_\perp^2 u_r + R^{1-\gamma_c}\theta^{1-\gamma_e}\partial_\perp^2 u_s \in L^2(\mathcal{V}_e^c)\\ R^{1-\gamma_c}\partial_\perp\partial_3 u = R^{1-\gamma_c}\partial_\perp\partial_3 u_r + R^{1-\gamma_c}\partial_\perp\partial_3 u_s \in L^2(\mathcal{V}_e^c)\\ R^{1-\gamma_c}\theta^{-\mu_e}\partial_3^2 u \in L^2(\mathcal{V}_e^c).\end{aligned}$$

Then, we have proved (30), (31), and (32). ∎

Remark 3.6 From the proof of Corollary 3.5, we see that we can take $\gamma_c = 1$ if $\lambda_c > 1/2$ and take $\gamma_e = 1$ if e is regular; and that the estimates (27) – (32) are also valid in $\mathcal{V}_e^0$ with R_c replaced by 1 and valid in $\mathcal{V}_c^0$ with $\theta_{c,e}$ replace by 1.

Consequently, we obtain the regularity estimates for equation (1) with $f \in L^2_{\boldsymbol{\mu}^*}(\Omega)$.

Corollary 3.7 *Recall the interior of the domain $\mathcal{V}^0$ in (8). Under the assumption of Lemma 3.2, for $f \in L^2_{\boldsymbol{\mu}^*}(\Omega)$ defined in (10), let $\gamma_e, \gamma_c \in [0,1]$ be such that $\mu_e^* \le \gamma_e < \lambda_e$, $\gamma_c < \lambda_c + 1/2$; and $\gamma_e = 1$ if $\lambda_e \ge 1$, $\gamma_c = 1$ if $\lambda_c > 1/2$. Define the weighted space*

$$\begin{aligned}\mathcal{H}^2_{\boldsymbol{\gamma}}(\Omega) := \{v \in H^2_{loc}(\Omega)|\ & R_c^{\gamma_e-\gamma_c}r_e^{-1-\gamma_e}v,\ R_c^{\gamma_e-\gamma_c}r_e^{-\gamma_e}\partial_\perp v,\ R_c^{1-\gamma_c}r_e^{-1}\partial_3 v \in L^2(\mathcal{V}_c^e),\\ & R_c^{\gamma_e-\gamma_c}r_e^{1-\gamma_e}\partial_\perp^2 v,\ R_c^{1-\gamma_c}\partial_\perp\partial_3 v,\ R_c^{1+\mu_e^*-\gamma_c}r_e^{-\mu_e^*}\partial_3^2 v \in L^2(\mathcal{V}_c^e);\\ & r_e^{-1-\gamma_e}v,\ r_e^{-\gamma_e}\partial_\perp v,\ r_e^{-1}\partial_3 v \in L^2(\mathcal{V}_e^0),\\ & r_e^{1-\gamma_e}\partial_\perp^2 v,\ \partial_\perp\partial_3 v,\ r_e^{-\mu_e^*}\partial_3^2 v \in L^2(\mathcal{V}_e^0);\\ & R_c^{-1-\gamma_c}v,\ R_c^{-\gamma_c}\partial_\perp v,\ R_c^{-\gamma_c}\partial_3 v \in L^2(\mathcal{V}_c^0),\\ & R_c^{1-\gamma_c}\partial_\perp^2 v,\ R_c^{1-\gamma_c}\partial_\perp\partial_3 v,\ R_c^{1-\gamma_c}\partial_3^2 v \in L^2(\mathcal{V}_c^0)\},\end{aligned}$$

with the norm

$$\|v\|^2_{\mathcal{H}^2_{\boldsymbol{\gamma}}(\Omega)} := \|v\|^2_{H^2(\mathcal{V}^0)} + \sum_{c\in\mathcal{C},e\in\mathcal{E}_c,} \Big(\|R_c^{1-\gamma_c}\theta_{c,e}^{-\mu_e^*}\partial_3^2 v\|^2_{L^2(\mathcal{V}_c^e)} + \sum_{|\alpha_\perp|=1} \|R_c^{1-\gamma_c}\partial^{\alpha_\perp}\partial_3 v\|^2_{L^2(\mathcal{V}_c^e)}$$
$$+\|R_c^{-\gamma_c}\theta_{c,e}^{-1}\partial_3 v\|^2_{L^2(\mathcal{V}_c^e)} + \sum_{|\alpha_\perp|\le 2} \|R_c^{|\alpha_\perp|-1-\gamma_c}\theta_{c,e}^{|\alpha_\perp|-1-\gamma_e}\partial^{\alpha_\perp} v\|^2_{L^2(\mathcal{V}_c^e)}\Big)$$
$$+ \sum_{c\in\mathcal{C},|\alpha|\le 2} \|R_c^{|\alpha|-1-\gamma_c}\partial^{\alpha} v\|^2_{L^2(\mathcal{V}_c^0)} + \sum_{e\in\mathcal{E}} \Big(\|r_e^{-\mu_e^*}\partial_3^2 v\|^2_{L^2(\mathcal{V}_e^0)}$$
$$+ \sum_{|\alpha_\perp|=1} \|\partial^{\alpha_\perp}\partial_3 v\|^2_{L^2(\mathcal{V}_e^0)} + \|r_e^{-1}\partial_3 v\|^2_{L^2(\mathcal{V}_e^0)} + \sum_{|\alpha_\perp|\le 2} \|r_e^{|\alpha_\perp|-1-\gamma_e}\partial^{\alpha_\perp} v\|^2_{L^2(\mathcal{V}_e^0)}\Big),$$

where ∂_3 is the derivative in the direction of e, $\partial^{\alpha_\perp} = \partial_1^{\alpha_1}\partial_2^{\alpha_2}$ for $\alpha_\perp = (\alpha_1,\alpha_2)$, and $\alpha = (\alpha_1,\alpha_2,\alpha_3)$. Then, the solution $u \in H_0^1(\Omega)$ of equation (1) satisfies

$$\|u\|_{\mathcal{H}^2_{\boldsymbol{\gamma}}(\Omega)} \le C\|f\|_{L^2_{\boldsymbol{\mu}^*}(\Omega)}. \tag{38}$$

Proof. The estimate (38) is a direct consequence of Corollary 3.5 and Remark 3.6. Corollary 3.5 holds for μ_e in (11) and for all $\gamma_e \in [0,1]$ and $\gamma_e < \lambda_e$. Thus, it still holds if we replace μ_e by μ_e^* and replace 0 by μ_e^* as the lower bound for γ_e. ■

4 Anisotropic finite element algorithms

In this section, we develop optimal FEMs approximating equation (1) with $f \in L^2_{\boldsymbol{\mu}^*}(\Omega)$. In particular, we give explicit values for the associated parameters in the algorithm, with which we shall prove the proposed method achieves the optimal rate of convergence, even when the solution is singular and the triangulation does not preserve the maximum angle condition.

Recall the vertex set $\mathcal{C}$ and the edge set $\mathcal{E}$. Following the notation in [23], we first classify tetrahedra in the triangulation of Ω.

Definition 4.1 *(Tetrahedron Types) Let T be a tetrahedron. If an edge e_T of T lies on $e \in \mathcal{E}$, we call e_T a marked edge. Let c_T be a vertex of T. If $c_T \in \mathcal{C}$, or if c_T is an interior point of an edge $e \in \mathcal{E}$ but does not belong to any marked edge, we call c_T a marked vertex. Let $\mathcal{T}$ be a tetrahedral triangulation of Ω, such that (I) each tetrahedron contains at most one marked vertex and at most one marked edge; (II) if a tetrahedron contains both a marked vertex and a marked edge, the marked vertex is an endpoint of the marked edge. Let $\mathcal{S} = \mathcal{E} \cup \mathcal{C}$. Then, there are five possible types for each tetrahedron $T \in \mathcal{T}$.*

1. *o-tetrahedron: $\bar{T} \cap \mathcal{S} = \emptyset$.*
2. *v-tetrahedron: $\bar{T} \cap \mathcal{S} = c \in \mathcal{C}$.*
3. *v_e-tetrahedron: $\bar{T} \cap \mathcal{S}$ is an interior point of an edge in $\mathcal{E}$.*
4. *e-tetrahedron: $\bar{T} \cap \mathcal{S}$ is a marked edge, but contains no vertex in $\mathcal{C}$.*
5. *ev-tetrahedron: $\bar{T} \cap \mathcal{S}$ contains a marked edge and a marked vertex.*

Then, for the reader's convenience, we recall the following anisotropic mesh algorithm [23].

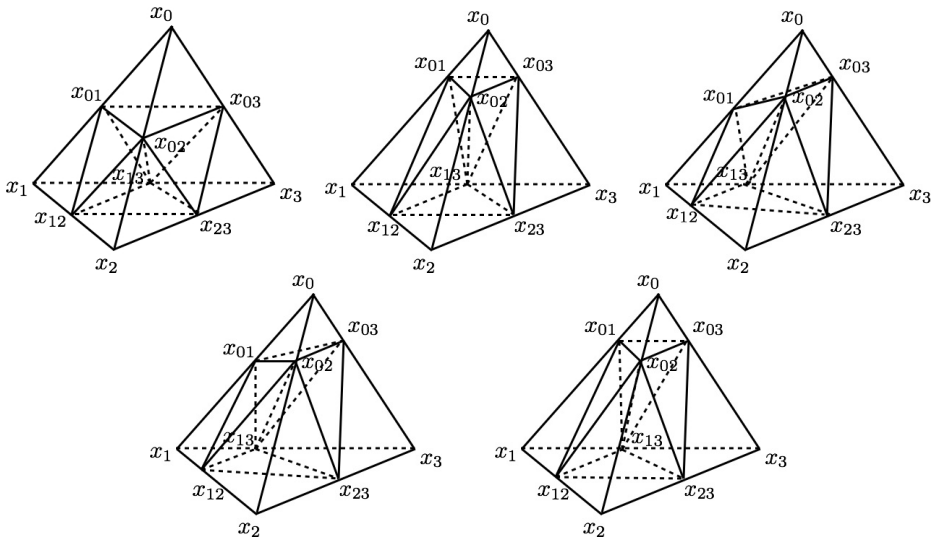

Figure 1: Refinements of a tetrahedron $\triangle^4 x_0x_1x_2x_3$, top (left – right): o-tetrahedron, v- or v_e-tetrahedron, e-tetrahedron; bottom (left – right): two ev-tetrahedra with $\kappa_{ec} = \kappa_e$ and $\kappa_{ec} = \kappa_c$.

Algorithme 4.2 *(Anisotropic Refinement) Let $\mathcal{T}$ be a triangulation of Ω as in Definition 4.1. To each $c \in \mathcal{C}$ (resp. $e \in \mathcal{E}$), we associate a grading parameter κ_c (resp. κ_e) $\in (0, 1/2]$. Let $T = \triangle^4 x_0x_1x_2x_3 \in \mathcal{T}$ be a tetrahedron with vertices x_0, x_1, x_2, x_3, such that x_0 is the marked vertex if T is a v-, v_e-, or ev-tetrahedron; and x_0x_1 is the marked edge if T is an e- or ev-tetrahedron. Let $\boldsymbol{\kappa}$ be the collection of the parameters κ_c and κ_e for all $c \in \mathcal{C}$ and $e \in \mathcal{E}$. Then, the refinement, denoted by $\boldsymbol{\kappa}(\mathcal{T})$, proceeds as follows. We first generate new nodes x_{kl}, $0 \le k < l \le 3$, on each edge x_kx_l of T, based on its type.*

(I) o-tetrahedron: $x_{kl} = (x_k + x_l)/2$.

(II) v-tetrahedron: Suppose $x_0 = c \in \mathcal{C}$. Define $\kappa = \kappa_{ec} := \min_{e \in \mathcal{E}_c}(\kappa_c, \kappa_e)$. Then, $x_{kl} = (x_k + x_l)/2$ for $1 \le k < l \le 3$; $x_{0l} = (1 - \kappa)x_0 + \kappa x_l$ for $1 \le l \le 3$.

(III) v_e-tetrahedron: Suppose x_0 is an interior point of $e \in \mathcal{E}$. Let $\kappa = \kappa_e$. Then, $x_{kl} = (x_k + x_l)/2$ for $1 \le k < l \le 3$; $x_{0l} = (1 - \kappa)x_0 + \kappa x_l$ for $1 \le l \le 3$.

(IV) e-tetrahedron: Suppose $x_0x_1 \subseteq e \in \mathcal{E}$. Then, $x_{kl} = (1 - \kappa_e)x_k + \kappa_e x_l$ for $0 \le k \le 1$ and $2 \le l \le 3$; $x_{01} = (x_0 + x_1)/2$, $x_{23} = (x_2 + x_3)/2$.

(V) ev-tetrahedron: Suppose $x_0 = c \in \mathcal{C}$ and $x_0x_1 \subseteq e \in \mathcal{E}_c$. Define $\kappa_{ec} := \min_{e \in \mathcal{E}_c}(\kappa_c, \kappa_e)$. Then, for $2 \le l \le 3$, $x_{0l} = (1 - \kappa_{ec})x_0 + \kappa_{ec}x_l$ and $x_{1l} = (1 - \kappa_e)x_1 + \kappa_e x_l$; $x_{01} = (1 - \kappa_c)x_0 + \kappa_c x_1$, $x_{23} = (x_2 + x_3)/2$.

Connecting these nodes x_{kl} on all the faces of T, we obtain four sub-tetrahedra and one octahedron. The octahedron then is cut into four tetrahedra using x_{13} as the common vertex. Therefore, after one refinement, we obtain eight sub-tetrahedra for each $T \in \mathcal{T}$ denoted by their vertices:

$$\triangle^4 x_0x_{01}x_{02}x_{03},\ \triangle^4 x_1x_{01}x_{12}x_{13},\ \triangle^4 x_2x_{02}x_{12}x_{23},\ \triangle^4 x_3x_{03}x_{13}x_{23},$$
$$\triangle^4 x_{01}x_{02}x_{03}x_{13},\ \triangle^4 x_{01}x_{02}x_{12}x_{13},\ \triangle^4 x_{02}x_{03}x_{13}x_{23},\ \triangle^4 x_{02}x_{12}x_{13}x_{23}.$$

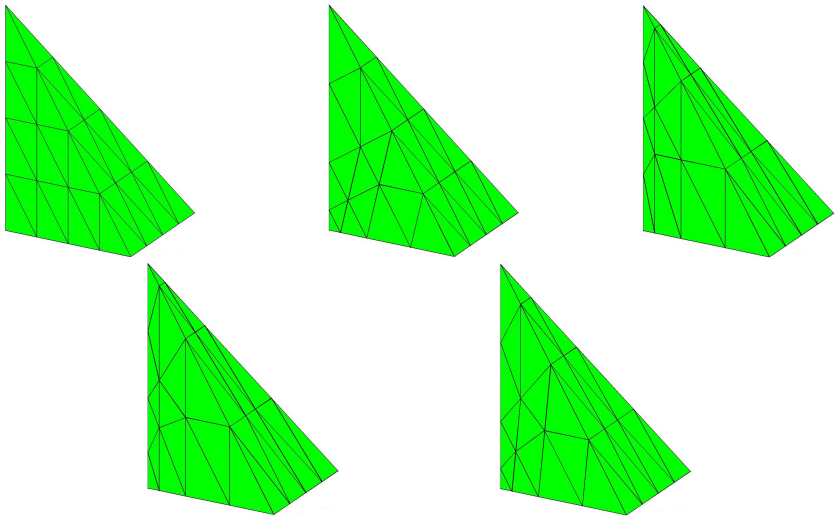

Figure 2: Anisotropic triangulations after two consecutive refinements on a tetrahedron, top (left – right): o-tetrahedron, v- or v_e-tetrahedron ($\kappa = 0.3$), e-tetrahedron ($\kappa_e = 0.3$); bottom (left – right): two ev-tetrahedra ($\kappa_{ec} = 0.3, \kappa_c = 0.4, \kappa_e = 0.3$) and ($\kappa_{ec} = 0.3, \kappa_v = 0.3, \kappa_e = 0.4$).

See Figure 1 for different types of decompositions. Given an initial mesh $\mathcal{T}_0$ satisfying the condition in Definition 4.1, the associated family of anisotropic meshes $\{\mathcal{T}_n,\ n \geq 0\}$ is defined recursively $\mathcal{T}_n = \boldsymbol{\kappa}(\mathcal{T}_{n-1})$. See Figure 2 for example.

Remark 4.3 *It is clear that different types of tetrahedra in Definition 4.1 are associated to different sub-regions of Ω in (7) and (8). The anisotropic mesh in Algorithm 4.2 is determined by the grading parameters κ_c and κ_e. A smaller value of the parameter leads to a higher mesh density near the vertex or the edge, while the value $\kappa_c = \kappa_e = 1/2$ corresponds to a quasi-uniform refinement. Therefore, in $\mathcal{V}^0$, the mesh is isotropic and quasi-uniform. The local refinement for a v- or v_e-tetrahedron in fact follows the same rule: the mesh is isotropic and graded toward the vertex x_0 based on the grading parameter κ associated to the vertex x_0. In $\mathcal{V}_e^0$, the resulting mesh in general is anisotropic and graded toward the edge $e \in \mathcal{E}$. The refinement in $\mathcal{V}_e^c$ depends on the parameters κ_c and κ_e, $e \in \mathcal{E}_c$, which is also anisotropic, graded toward the edge $e \in \mathcal{E}$ and the vertex $c \in \mathcal{C}$.*

Now, we proceed to propose our finite element algorithm for equation (1) with $f \in L^2_{\boldsymbol{\mu}^*}(\Omega)$.

Algorithme 4.4 *(Anisotropic Finite Element Algorithm) Let $\mathcal{T}_0$ be the initial triangulation of Ω that satisfy the condition in Definition 4.1. Then, each parameter κ_c (resp. κ_e) $\in (0, 1/2]$ is uniquely determined by a new parameter a_c (resp. a_e) $\in (0, 1]$, such that*

$$\kappa_c = 2^{-1/a_c} \quad \text{and} \quad \kappa_e = 2^{-1/a_e}. \tag{39}$$

Let $a_{ec} := \min_{e \in \mathcal{E}_c}(a_c, a_e)$. Then, κ_{ec} is determined by a_{ec} via

$$\kappa_{ec} = 2^{-1/a_{ec}}. \tag{40}$$

Recall γ_c, γ_e, and μ_e^* in Corollary 3.7. We choose a_c and a_e, such that

$$1-\mu_e^* \le a_e \le \mu_e^* \quad \text{if } e \text{ is singular;} \qquad a_e = 1 \quad \text{if } e \text{ is regular;} \tag{41}$$

$$a_C := 2 + a_{ec} - \tfrac{2a_{ec}}{a_c} \le \gamma_c. \tag{42}$$

Let $\mathcal{T}_n$ be the mesh obtained after n anisotropic refinements (Algorithm 4.2) from $\mathcal{T}_0$ based on the parameters κ_c and κ_e defined by a_e and a_c through (39) – (42). Then, the linear finite element approximation u_n to equation (1) is defined by (3) on the mesh $\mathcal{T}_n$.

Remark 4.5 *Based on (42), $a_C \ge a_c \ge a_{ec}$, with the equal sign being taken when $a_c = a_{ec}$. By choosing a_e close to μ_e^* and a_c small, it is clear that the conditions (41) and (42) lead to a non-empty set. Note further that if c is a regular vertex ($\gamma_c = 1$), the condition (42) becomes*

$$a_c \le \frac{2a_{ec}}{1+a_{ec}}.$$

Hence the choice $a_c = 1$ leads to $a_{ec} = 1$. In other words, the choice ($a_c = 1$) is only possible if all the edges of $\mathcal{E}_c$ are also regular; otherwise the simplest choice is to take $a_c \le a_e$, for all $e \in \mathcal{E}_c$, leading to $a_c = a_{ec}$.

For $0 < a_e < 1$, it is clear that refinements for an e- or ev-tetrahedron lead to anisotropic meshes toward the edge that do not preserve the maximum angle condition. Namely, the maximum edge angle in the face of the tetrahedron approaches π as the level of refinement n increases. This is a main difficulty that we shall overcome in the error analysis.

5 Finite element error analysis

In this section, we provide detailed interpolation error analysis for the finite element algorithm proposed in the previous section. Using these local error estimates, we shall show that Algorithm 4.4 gives rise to numerical solutions that converge in the H^1 norm to the singular solution in the optimal rate.

Recall that under the condition in Corollary 3.7, when the given data $f \in L^2_{\boldsymbol{\mu}^*}(\Omega)$, the solution $u \in H^2_{\boldsymbol{\gamma}}(\Omega)$. The space $\mathcal{H}^2_{\boldsymbol{\gamma}}$ is equivalent to H^2 on any sub-region of Ω that is away from $\mathcal{E} \cup \mathcal{C}$. Therefore, by the Sobolev embedding Theorem, the solution u is continuous in the interior of the domain. For a given mesh, we define the Lagrange interpolation u_I of u such that $u_I = u$ at the interior nodes and $u_I = 0$ on the boundary.

Note that the tetrahedra in the initial mesh $\mathcal{T}_0 = \{T_{(0),j}\}_{j=1}^J$ are all shape regular and can be classified into five categories (Definition 4.1). Then, we carry out the interpolation error analysis on different sub-regions of Ω, each of which is represented by an initial tetrahedron in $\mathcal{T}_0$. Due to the different weighted space for the solution ($u \in H^2_{\boldsymbol{\gamma}}(\Omega)$) and different selection criteria for the mesh parameters in (41) – (42), the error estimates in [23] do not extend to the problem in this paper. However, some notation (e.g., mesh layers) and intermediate results established in [23] will be recalled when it is necessary to simplify the exposition and to make the analysis self-contained.

5.1 Estimates on initial o-, v-, and v_e-tetrahedra in $\mathcal{T}_0$

We first have the estimate for an o-tetrahedron in the initial mesh.

Lemma 5.1 *Let $T_{(0)} \in \mathcal{T}_0$ be an o-tetrahedron. For $u \in \mathcal{H}^2_{\boldsymbol{\gamma}}(\Omega)$, let u_I be its nodal interpolation on $\mathcal{T}_n$. Then, we have*

$$|u - u_I|_{H^1(T_{(0)})} \le Ch\|u\|_{\mathcal{H}^2_{\boldsymbol{\gamma}}(T_{(0)})}, \tag{43}$$

where $h = 2^{-n}$ and C is independent of n and u.

Proof. Based on Algorithm 4.2, the restriction of $\mathcal{T}_n$ on $T_{(0)}$ is a quasi-uniform mesh with size $O(2^{-n})$. Since H^2 is equivalent to $\mathcal{H}^2_{\boldsymbol{\gamma}}$ on an o-tetrahedron, by the standard interpolation error estimate, we obtain

$$|u - u_I|_{H^1(T_{(0)})} \le C2^{-n}\|u\|_{H^2(T_{(0)})} \le Ch\|u\|_{\mathcal{H}^2_{\boldsymbol{\gamma}}(T_{(0)})}.$$

■

For a v- or v_e-tetrahedron in $\mathcal{T}_0$, we first identify its subsets that have comparable distances to the marked vertex.

Definition 5.2 *(Mesh Layers in v- and v_e-tetrahedra) Let $T_{(0)} = \triangle^4 x_0x_1x_2x_3 \in \mathcal{T}_0$ be either a v- or a v_e-tetrahedron with $x_0 \in \mathcal{C}$ or $x_0 \in e \in \mathcal{E}$. We use a local Cartesian coordinate system, such that x_0 is the origin. For $1 \le i \le n$, the ith refinement on $T_{(0)}$ produces a small tetrahedron with x_0 as a vertex and with one face, denoted by $P_{v,i}$, parallel to the face $\triangle^3 x_1x_2x_3$ of $T_{(0)}$. See Figure 1 for example. Then, after n refinements, we define the ith mesh layer $L_{v,i}$ of $T_{(0)}$, $1 \le i < n$, as the region in $T_{(0)}$ between $P_{v,i}$ and $P_{v,i+1}$. We denote by $L_{v,0}$ the region in $T_{(0)}$ between $\triangle^3 x_1x_2x_3$ and $P_{v,1}$; and let $L_{v,n}$ be the small tetrahedron with x_0 as a vertex that is bounded by $P_{v,n}$ and three faces of $T_{(0)}$. Since x_0 is the only point for the special refinement, we drop the sub-index in the grading parameter. Namely, for such $T_{(0)}$, we use*

$$\kappa = 2^{-1/a}$$

to denote the grading parameter near x_0 ($\kappa = \kappa_{ec}$ if $x_0 \in \mathcal{C}$ and $\kappa = \kappa_e$ if $x_0 \in e \in \mathcal{E}$). Then, by Algorithm 4.2, the dilation matrix

$$\mathbf{B}_{v,i} := \begin{pmatrix} \kappa^{-i} & 0 & 0 \\ 0 & \kappa^{-i} & 0 \\ 0 & 0 & \kappa^{-i} \end{pmatrix} \tag{44}$$

maps $L_{v,i}$ to $L_{v,0}$ for $0 \le i < n$, and maps $L_{v,n}$ to $T_{(0)}$. We define the initial triangulation of $L_{v,i}$, $0 \le i < n$, to be the first decomposition of $L_{v,i}$ into tetrahedra. Thus, the initial triangulation of $L_{v,i}$ consists of those tetrahedra in $\mathcal{T}_{i+1}$ that are contained in the layer $L_{v,i}$.

Remark 5.3 *Based on the refinement, on $L_{v,i}$, $0 \le i \le n$, the tetrahedra in $\mathcal{T}_n$ are isotropic with mesh size $O(\kappa^i 2^{i-n})$. In $T_{(0)}$, let ρ be the distance to x_0. Therefore,*

$$\rho \sim \kappa^i \qquad \text{on } L_{v,i}, \quad 0 \le i < n. \tag{45}$$

Namely, if $T_{(0)}$ is a v-tetrahedron, $\rho \sim R_c$ for $c = x_0 \in \mathcal{C}$; and if $T_{(0)}$ is a v_e-tetrahedron, $\rho \sim r_e$, where $e \in \mathcal{E}$ is the edge containing x_0.

Then, we have the interpolation error estimate in the layer $L_{v,i}$.

Lemma 5.4 *Let $T_{(0)} \in \mathcal{T}_0$ be either a v- or a v_e-tetrahedron. For $u \in \mathcal{H}^2_{\boldsymbol{\gamma}}(\Omega)$, let u_I be its nodal interpolation on $\mathcal{T}_n$. Then, for $0 \le i < n$, we have*

$$|u - u_I|_{H^1(L_{v,i})} \le Ch\|u\|_{\mathcal{H}^2_{\boldsymbol{\gamma}}(L_{v,i})},$$

where $h = 2^{-n}$ and C is independent of i and u.

Proof. For $(x, y, z) \in L_{v,i}$, let $(\hat{x}, \hat{y}, \hat{z}) \in L_{v,0}$ be its image under the dilation $\mathbf{B}_{v,i}$ in (44). For a function v on $L_{v,i}$, we define $\hat{v}$ on $L_{v,0}$ by

$$\hat{v}(\hat{x}, \hat{y}, \hat{z}) := v(x, y, z).$$

As part of $\mathcal{T}_n$, the triangulation on $L_{v,i}$ is mapped by $\mathbf{B}_{v,i}$ to a triangulation on $L_{v,0}$ with mesh size $O(2^{i-n})$. Then, by the scaling argument, we have

$$\begin{aligned} |u - u_I|^2_{H^1(L_{v,i})} &= \kappa^i |\hat{u} - \hat{u}_I|^2_{H^1(L_{v,0})} \le C\kappa^i 2^{2(i-n)} |\hat{u}|^2_{H^2(L_{v,0})} \\ &\le C 2^{2(i-n)} \kappa^{2i} |u|^2_{H^2(L_{v,i})}. \end{aligned}$$

If $T_{(0)}$ is a v-tetrahedron, we have $R_c \sim \kappa^i = \kappa^i_{ec}$ on $L_{v,i}$ and $a_{ec} \le a_C \le \gamma_c$. Therefore, by (40), we have

$$2^{2(i-n)}\kappa^{2i}|u|^2_{H^2(L_{v,i})} \le C2^{2(i-n)}\kappa_{ec}^{2ia_{ec}} \sum_{|\alpha|=2} \|R_c^{1-a_{ec}}\partial^\alpha u\|^2_{L^2(L_{v,i})} \le C2^{-2n}\|u\|^2_{\mathcal{H}^2_{\boldsymbol{\gamma}}(L_{i,v})}.$$

If $T_{(0)}$ is a v_e-tetrahedron, we have $r_e \sim \kappa^i = \kappa^i_e$ on $L_{v,i}$. By (39), (41), and $\mu^*_e \le \gamma_e \le 1$ (Corollary 3.7), we have

$$\begin{aligned} 2^{2(i-n)}\kappa^{2i}|u|^2_{H^2(L_{v,i})} &\le C2^{2(i-n)}\kappa_e^{2ia_e} \sum_{|\alpha|=2} \|r_e^{1-a_e}\partial^\alpha u\|^2_{L^2(L_{v,i})} \\ &\le C2^{-2n}\Big(\sum_{|\alpha_\perp|=2} \|r_e^{1-a_e}\partial^{\alpha_\perp} u\|^2_{L^2(L_{v,i})} + \sum_{|\alpha_\perp|=1} \|\partial^{\alpha_\perp}\partial_z u\|^2_{L^2(L_{v,i})} + \|r_e^{-a_e}\partial_z^2 u\|^2_{L^2(L_{v,i})}\Big) \\ &\le C2^{-2n}\|u\|^2_{\mathcal{H}^2_{\boldsymbol{\gamma}}(L_{i,v})}. \end{aligned}$$

Therefore, in both cases, we have

$$|u - u_I|^2_{H^1(L_{v,i})} \le C2^{-2n}\|u\|^2_{\mathcal{H}^2_{\boldsymbol{\gamma}}(L_{i,v})} = Ch^2\|u\|^2_{\mathcal{H}^2_{\boldsymbol{\gamma}}(L_{i,v})},$$

which completes the proof. ■

Then, we give the error estimate on the whole initial tetrahedron $T_{(0)}$.

Corollary 5.5 *Let $T_{(0)} \in \mathcal{T}_0$ be either a v- or a v_e-tetrahedron. For $u \in \mathcal{H}^2_{\boldsymbol{\gamma}}(\Omega)$, let u_I be its nodal interpolation on $\mathcal{T}_n$. Then, we have*

$$|u - u_I|_{H^1(T_{(0)})} \le Ch\|u\|_{\mathcal{H}^2_{\boldsymbol{\gamma}}(T_{(0)})},$$

where $h = 2^{-n}$ and C is independent of n and u.

Proof. By Lemma 5.4, it suffices to show the estimate for the last layer $L_{v,n}$. For $(x,y,z) \in L_{v,n}$, let $(\hat{x},\hat{y},\hat{z}) \in T_{(0)}$ be its image under the dilation $\mathbf{B}_{v,n}$. For a function v on $L_{v,n}$, we define $\hat{v}$ on $T_{(0)}$ by

$$\hat{v}(\hat{x},\hat{y},\hat{z}) := v(x,y,z).$$

Now, let χ be a smooth cutoff function on $T_{(0)}$, such that $\chi = 0$ in a neighborhood of x_0 and $= 1$ at every other node of $T_{(0)}$. Recall the distance function ρ from (45). Thus, $\rho(\hat{x},\hat{y},\hat{z}) = \kappa^{-n}\rho(x,y,z)$. Since $\chi\hat{u} = 0$ in the neighborhood of x_0, we have

$$|\chi\hat{u}|^2_{H^2(T_{(0)})} \le C \sum_{|\alpha|\le 2} \|\rho^{|\alpha|-1}\partial^\alpha \hat{u}\|^2_{L^2(T_{(0)})}. \tag{46}$$

Define $\hat{w} := \hat{u} - \chi\hat{u}$ and note that $(\chi\hat{u})_I = \hat{u}_I$. We have

$$\begin{aligned} |\hat{u} - \hat{u}_I|_{H^1(T_{(0)})} &= |\hat{w} + \chi\hat{u} - \hat{u}_I|_{H^1(T_{(0)})} \le |\hat{w}|_{H^1(T_{(0)})} + |\chi\hat{u} - \hat{u}_I|_{H^1(T_{(0)})} \\ &= |\hat{w}|_{H^1(T_{(0)})} + |\chi\hat{u} - (\chi\hat{u})_I|_{H^1(T_{(0)})} \le C(\|\hat{u}\|_{H^1(T_{(0)})} + |\chi\hat{u}|_{H^2(T_{(0)})}), \end{aligned} \tag{47}$$

where C depends only on $T_{(0)}$. Then, using (47), (46), the scaling argument, and $\kappa^{-n} \lesssim \rho^{-1}$ in $L_{v,n}$, we have

$$\begin{aligned} |u - u_I|^2_{H^1(L_{v,n})} &= \kappa^n |\hat{u} - \hat{u}_I|^2_{H^1(T_{(0)})} \le C\kappa^n(\|\hat{u}\|^2_{H^1(T_{(0)})} + \sum_{|\alpha|\le 2} \|\rho^{|\alpha|-1}\partial^\alpha \hat{u}\|^2_{L^2(T_{(0)})}) \\ &\le C \sum_{|\alpha|\le 2} \|\rho^{|\alpha|-1}\partial^\alpha u\|^2_{L^2(L_{v,n})} \le C\kappa^{2na} \sum_{|\alpha|\le 2} \|\rho^{|\alpha|-1-a}\partial^\alpha u\|^2_{L^2(L_{v,n})}. \end{aligned}$$

When $T_{(0)}$ is a v-tetrahedron, by $\rho \sim R_c$, the definition of the weighted space, (40), the inequality $a_{ec} \le a_C$, and (42), we have

$$|u - u_I|^2_{H^1(L_{v,n})} \le C2^{-2n} \sum_{|\alpha|\le 2} \|R_c^{|\alpha|-1-a_{ec}}\partial^\alpha u\|^2_{L^2(L_{v,n})} \le Ch^2\|u\|^2_{\mathcal{H}^2_\gamma(L_{v,n})}.$$

When $T_{(0)}$ is a v_e-tetrahedron, by $\rho \sim r_e$, the definition of the weighted space, (39), and (41), one obtains

$$\begin{aligned} |u - u_I|^2_{H^1(L_{v,n})} &\le C2^{-2n} \sum_{|\alpha|\le 2} \|r_e^{|\alpha|-1-a_e}\partial^\alpha u\|^2_{L^2(L_{v,n})} \\ &\le Ch^2(\|r_e^{-1}\partial_z u\|^2_{L^2(L_{v,n})} + \|r_e^{-a_e}\partial_z^2 u\|^2_{L^2(L_{v,n})} + \sum_{|\alpha_\perp|=1} \|\partial^{\alpha_\perp}\partial_z u\|^2_{L^2(L_{v,n})} \\ &\quad + \sum_{|\alpha_\perp|\le 2} \|r_e^{|\alpha_\perp|-1-a_e}\partial^{\alpha_\perp} u\|^2_{L^2(L_{v,n})}) \le Ch^2\|u\|^2_{\mathcal{H}^2_\gamma(L_{v,n})}. \end{aligned}$$

Then, the desired estimate follows by summing up the estimates from layers $L_{v,i}$, $0 \le i \le n$. ∎

5.2 Estimates on initial e-tetrahedra in $\mathcal{T}_0$

Throughout this subsection, let $T_{(0)} := \triangle^4 x_0x_1x_2x_3 \in \mathcal{T}_0$ be an e-tetrahedron with $x_0x_1 \subset e \in \mathcal{E}$. Then, we first define the mesh layer associated with $\mathcal{T}_n$ on $T_{(0)}$.

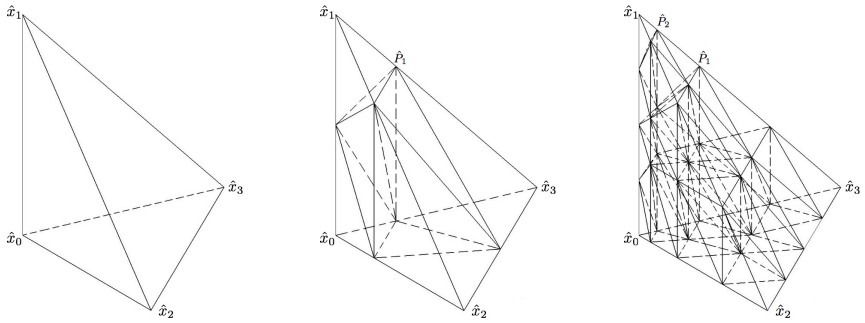

Figure 3: A reference tetrahedron $\hat{T}$ (left); the triangulation $\hat{\mathcal{T}}_1$ after one edge refinement (center); the triangulation $\hat{\mathcal{T}}_2$ after two edge refinements (right).

Definition 5.6 *(Mesh Layers in e-tetrahedra) Based on Algorithm 4.2, in each refinement, an e-tetrahedron is cut by a parallelogram parallel to x_0x_1. For example, in the e-tetrahedron of Figure 1, the quadrilateral with vertices $x_{02}, x_{12}, x_{13}, x_{03}$ is the aforementioned parallelogram. We denote by $P_{e,i}$ the parallelogram produced in the ith refinement, $1 \le i \le n$. For the mesh $\mathcal{T}_n$, let the ith layer $L_{e,i}$ on $T_{(0)}$, $0 < i < n$, be the region bounded by $P_{e,i}$, $P_{e,i+1}$, and the faces of $T_{(0)}$. Define $L_{e,0}$ to be the sub-region of $T_{(0)}$ away from e that is separated by $P_{e,1}$. Define $L_{e,n}$ to be the sub-region of $T_{(0)}$ between $P_{e,n}$ and e. See also Figure 3. As in Definition 5.2, the initial triangulation of the layer $L_{e,i}$, $0 \le i < n$, consists of the tetrahedra in $\mathcal{T}_{i+1}$ that are contained in $L_{e,i}$. Therefore,*

$$r_e \sim \kappa_e^i \quad \text{on } L_{e,i},\ 0 \le i < n. \tag{48}$$

Then, we define the reference element for the e-tetrahedron.

Definition 5.7 *(The Reference e-tetrahedron) For the initial e-tetrahedron $T_{(0)} := \triangle^4 x_0x_1x_2x_3 \in \mathcal{T}_0$, we use a local Cartesian coordinate system, such that the z-axis contains the edge x_0x_1 with the direction of $\overrightarrow{x_0x_1}$ as the positive direction, and x_2 is in the xz-plane. Let $l_0 := |x_0x_1|$ be the length of the marked edge. Then, we define the reference tetrahedron $\hat{T} = \triangle^4 \hat{x}_0\hat{x}_1\hat{x}_2\hat{x}_3$, such that*

$$\hat{x}_0 = (0, 0, -l_0/2), \quad \hat{x}_1 = (0, 0, l_0/2), \quad \hat{x}_k = (\hat{\lambda}_k, \hat{\xi}_k, -l_0/2),\ k = 2, 3, \tag{49}$$

where $\hat{\lambda}_k, \hat{\xi}_k$ are the x- and y-coordinates of the vertices x_2 and x_3, respectively. Therefore, $\hat{\xi}_2 = 0$ and $\hat{\lambda}_2, \hat{\lambda}_3, \hat{\xi}_3$ are constants that depend on the shape regularity of $T_{(0)}$. Thus, $\hat{T}$ is a tetrahedron with one face in the plane $z = -l_0/2$, one face in the xz-plane, such that $|\hat{x}_0\hat{x}_1| = |x_0x_1|$, $|\hat{x}_0\hat{x}_2| =$ the length of the orthogonal projection of x_0x_2 in the plane $z = -l_0/2$, and $|\hat{x}_0\hat{x}_3| =$ the length of the orthogonal projection of x_0x_3 in the plane $z = -l_0/2$. In addition, denote by $\hat{\mathcal{T}}_1$ and $\hat{\mathcal{T}}_2$ the triangulations of $\hat{T}$ after one and two edge refinements with the parameter κ_e to $\hat{x}_0\hat{x}_1$, respectively (see Figure 3).

For an e-tetrahedron $\mathcal{T}_i \ni T_{(i)} := \triangle^4 \gamma_0\gamma_1\gamma_2\gamma_3 \subset T_{(0)}$, $1 \le i \le n$, we define the $T_{(i)}$-based local coordinate system as follows. Let $\gamma_0\gamma_1$ be the marked edge, such that $\overrightarrow{\gamma_0\gamma_1}$ and $\overrightarrow{x_0x_1}$ share the same direction. We use the local coordinate system in Definition 5.7, and set $(\gamma_0 + \gamma_1)/2$ to be the origin. Recall the reference e-tetrahedron $\hat{T}$, and its triangulations $\hat{\mathcal{T}}_1$ and $\hat{\mathcal{T}}_2$ in Definition 5.7. Then, the following mappings to the reference element can be constructed (Lemma 4.15 in [23]).

Proposition 5.8 *Let $T_{(i+1)} \in \mathcal{T}_{i+1}$ be a tetrahedron, such that $T_{(i+1)} \subset L_{e,i} \subset T_{(0)}$, $0 \le i < n$. Case I: $T_{(i+1)}$ is contained in an e-tetrahedron $T_{(i)} \in \mathcal{T}_i$. Using the $T_{(i)}$-based local coordinate system, there is a transformation*

$$\mathbf{B}_{e,i} = \begin{pmatrix} \kappa_e^{-i} & 0 & 0 \\ 0 & \kappa_e^{-i} & 0 \\ b_1\kappa_e^{-i} & b_2\kappa_e^{-i} & 2^i \end{pmatrix} \tag{50}$$

that maps $T_{(i+1)}$ to one of the four o-tetrahedra in $\hat{\mathcal{T}}_1$ (hence, we have finitely many reference elements for all $T_{(i+1)}$). For an e-tetrahedron in the last layer $T_{(n)} \subset L_{e,n} \subset T_{(0)}$, using the $T_{(n)}$-based local coordinate system, there exists a transformation $\mathbf{B}_{e,n}$ of the form (50) with $i = n$ that maps $T_{(n)}$ to the reference tetrahedron $\hat{T}$.
Case II: $T_{(i+1)}$ is contained in a v_e-tetrahedron $T_{(i)} \in \mathcal{T}_i$. Let $T_{(k)} \in \mathcal{T}_k$, $1 \le k \le i$, be the v_e-tetrahedron, such that $T_{(i)} \subseteq T_{(k)}$ and $T_{(k)}$ is contained in an e-tetrahedron $T_{(k-1)} \in \mathcal{T}_{k-1}$. Using the $T_{(k-1)}$-based local coordinate system, there is a transformation

$$\mathbf{B}_{i,k} = \begin{pmatrix} \kappa_e^{-i+1} & 0 & 0 \\ 0 & \kappa_e^{-i+1} & 0 \\ b_1\kappa_e^{-i+1} & b_2\kappa_e^{-i+1} & 2^{k-1}\kappa_e^{k-i} \end{pmatrix} \tag{51}$$

that maps $T_{(i+1)}$ to one of the o-tetrahedra in $\hat{\mathcal{T}}_2$ (as in Case I, we again have finitely many reference elements for all $T_{(i+1)}$). For a v_e-tetrahedron in the last layer $T_{(n)} \subset L_{e,n} \subset T_{(0)}$, let $T_{(k)} \in \mathcal{T}_k$ be the v_e-tetrahedron, such that $T_{(n)} \subseteq T_{(k)}$ and $T_{(k)}$ is contained in an e-tetrahedron $T_{(k-1)} \in \mathcal{T}_{k-1}$. Using the $T_{(k-1)}$-based local coordinate system, there exists a transformation $\mathbf{B}_{n,k}$ of the form (51) with $i = n$ that maps $T_{(n)}$ to a v_e-tetrahedron in $\hat{\mathcal{T}}_1$.

In both cases, $|b_1|, |b_2| \le C_0$, for $C_0 > 0$ depending on $T_{(0)}$ but not on i, n, or k.

Each tetrahedron in $\mathcal{T}_{i+1}$ that belongs to the layer $L_{e,i}$, $0 \le i < n$, falls into either Case I or Case II of Proposition 5.8. Thus, there is a linear transformation $\mathbf{B}$ (either $\mathbf{B}_{e,i}$ or $\mathbf{B}_{i,k}$) that maps $T_{(i+1)}$ to an o-tetrahedron in either $\hat{\mathcal{T}}_1$ or in $\hat{\mathcal{T}}_2$. We denote this reference o-tetrahedron by $\hat{T}_{(i+1)}$. It is clear that $\hat{T}_{(i+1)}$ belongs to a finite number of similarity classes determined by the o-tetrahedra in $\hat{\mathcal{T}}_1$ and $\hat{\mathcal{T}}_2$. Then, for $(x, y, z) \in T_{(i+1)}$, we have

$$\mathbf{B}(x, y, z) = (\hat{x}, \hat{y}, \hat{z}) \in \hat{T}_{(i+1)}. \tag{52}$$

For a function v on $T_{(i+1)}$, we define $\hat{v}(\hat{x}, \hat{y}, \hat{z}) := v(x, y, z)$.

In the $(i+1)$st refinement, $0 \le i < n$, when the layer $L_{e,i}$ is formed, it only contains tetrahedra in $\mathcal{T}_{i+1}$. To obtain the mesh $\mathcal{T}_n$, these tetrahedra in $L_{e,i}$ are further refined uniformly $n - i - 1$ times. Thus, the mapping $\mathbf{B}$ maps $\mathcal{T}_n$ on $T_{(i+1)}$ to a quasi-uniform triangulation on $\hat{T}_{(i+1)}$ with mesh size $O(2^{i-n})$. Now, we obtain a uniform interpolation error estimate in the layer $L_{e,i}$.

Theorem 5.9 *Let $T_{(0)} \in \mathcal{T}_0$ be an e-tetrahedron and let u_I be its nodal interpolation on $\mathcal{T}_n$. Then, for $0 \le i < n$, we have*

$$|u - u_I|_{H^1(L_{e,i})} \le Ch\|u\|_{\mathcal{H}^2_\gamma(L_{e,i})},$$

where $L_{e,i}$ is the mesh layer in Definition 5.6, $h = 2^{-n}$, and C depends on $T_{(0)}$, but not on i.

Proof. Based on Algorithm 4.2, the layer $L_{e,i}$ is formed in the $(i+1)$st refinement and is the union of tetrahedra in $\mathcal{T}_{i+1}$ between $P_{e,i}$ and $P_{e,i+1}$. Therefore, it suffices to verify the following interpolation error estimate on each tetrahedron $\mathcal{T}_{i+1} \ni T_{(i+1)} \subset L_{e,i}$,

$$|u - u_I|_{H^1(T_{(i+1)})} \leq Ch\|u\|_{\mathcal{H}^2_{\vec{\gamma}}(T_{(i+1)})}. \tag{53}$$

Let $T_{(i)} \in \mathcal{T}_i$ be the tetrahedron containing $T_{(i+1)}$. Then, $T_{(i)}$ is either an e-tetrahedron or a v_e-tetrahedron. We show (53) based on $T_{(i)}$'s type.

Case I: $T_{(i)}$ is an e-tetrahedron. Let $(x,y,z) \in T_{(i+1)}$ and $(\hat{x},\hat{y},\hat{z}) \in \hat{T}_{(i+1)}$ as defined in (52). Then, by the mapping in (50), we have

$$\begin{cases} dxdydz = 2^{-i}\kappa_e^{2i} d\hat{x}d\hat{y}d\hat{z}; \\ \partial_x v = (\kappa_e^{-i}\partial_{\hat{x}} + b_1\kappa_e^{-i}\partial_{\hat{z}})\hat{v}, \quad \partial_y v = (\kappa_e^{-i}\partial_{\hat{y}} + b_2\kappa_e^{-i}\partial_{\hat{z}})\hat{v}, \quad \partial_z v = 2^i\partial_{\hat{z}}\hat{v}; \\ \partial_{\hat{x}}\hat{v} = (\kappa_e^{i}\partial_x - b_1 2^{-i}\partial_z)v, \quad \partial_{\hat{y}}\hat{v} = (\kappa_e^{i}\partial_y - b_2 2^{-i}\partial_z)v, \quad \partial_{\hat{z}}\hat{v} = 2^{-i}\partial_z v. \end{cases} \tag{54}$$

Therefore, by Proposition 5.8, (54), and the standard interpolation estimate on $\hat{T}_{(i+1)}$, we have

$$\begin{aligned} \|\partial_x(u-u_I)\|^2_{L^2(T_{(i+1)})} &\leq C2^{-i}\big(\|\partial_{\hat{x}}(\hat{u}-\hat{u}_I)\|^2_{L^2(\hat{T}_{(i+1)})} + \|\partial_{\hat{z}}(\hat{u}-\hat{u}_I)\|^2_{L^2(\hat{T}_{(i+1)})}\big) \\ &\leq C2^{-i}2^{2(i-n)}|\hat{u}|^2_{H^2(\hat{T}_{(i+1)})} \\ &\leq C2^{2(i-n)} \sum_{|\alpha_\perp|+\alpha_3=2} 2^{-2i\alpha_3}\kappa_e^{2i(|\alpha_\perp|-1)}\|\partial^{\alpha_\perp}\partial_z^{\alpha_3}u\|^2_{L^2(T_{(i+1)})}. \end{aligned} \tag{55}$$

A similar calculation for the derivative with respect to y gives

$$\|\partial_y(u-u_I)\|^2_{L^2(T_{(i+1)})} \leq C2^{2(i-n)} \sum_{|\alpha_\perp|+\alpha_3=2} 2^{-2i\alpha_3}\kappa_e^{2i(|\alpha_\perp|-1)}\|\partial^{\alpha_\perp}\partial_z^{\alpha_3}u\|^2_{L^2(T_{(i+1)})}. \tag{56}$$

In the z-direction, by Proposition 5.8, (54), and $\kappa_e \leq 1/2$, following the calculation in (55), we have

$$\begin{aligned} \|\partial_z(u-u_I)\|^2_{L^2(T_{(i+1)})} &\leq C2^{i}\kappa_e^{2i}\|\partial_{\hat{z}}(\hat{u}-\hat{u}_I)\|^2_{L^2(\hat{T}_{(i+1)})} \\ &\leq C2^{-i}\big(\|\partial_{\hat{x}}(\hat{u}-\hat{u}_I)\|^2_{L^2(\hat{T}_{(i+1)})} + \|\partial_{\hat{z}}(\hat{u}-\hat{u}_I)\|^2_{L^2(\hat{T}_{(i+1)})}\big) \\ &\leq C2^{2(i-n)} \sum_{|\alpha_\perp|+\alpha_3=2} 2^{-2i\alpha_3}\kappa_e^{2i(|\alpha_\perp|-1)}\|\partial^{\alpha_\perp}\partial_z^{\alpha_3}u\|^2_{L^2(T_{(i+1)})}. \end{aligned} \tag{57}$$

Thus, by (55) – (57), the estimate of the term

$$E := 2^{2(i-n)} \sum_{|\alpha_\perp|+\alpha_3=2} 2^{-2i\alpha_3}\kappa_e^{2i(|\alpha_\perp|-1)}\|\partial^{\alpha_\perp}\partial_z^{\alpha_3}u\|^2_{L^2(T_{(i+1)})}$$

is important for the error analysis. By (39) and (48), we first have

$$\begin{aligned} E &\leq C2^{-2n}(2^{-2i}\kappa_e^{-2i}\|\partial_z^2 u\|^2_{L^2(T_{(i+1)})} + \sum_{|\alpha_\perp|=1}\|\partial^{\alpha_\perp}\partial_z u\|^2_{L^2(T_{(i+1)})} + 2^{2i}\kappa_e^{2i}\sum_{|\alpha_\perp|=2}\|\partial^{\alpha_\perp}u\|^2_{L^2(T_{(i+1)})}) \\ &\leq Ch^2(\kappa_e^{2i(a_e-1)}\|\partial_z^2 u\|^2_{L^2(T_{(i+1)})} + \sum_{|\alpha_\perp|=1}\|\partial^{\alpha_\perp}\partial_z u\|^2_{L^2(T_{(i+1)})} + \kappa_e^{2i(1-a_e)}\sum_{|\alpha_\perp|=2}\|\partial^{\alpha_\perp}u\|^2_{L^2(T_{(i+1)})}) \\ &\leq Ch^2(\|r_e^{a_e-1}\partial_z^2 u\|^2_{L^2(T_{(i+1)})} + \sum_{|\alpha_\perp|=1}\|\partial^{\alpha_\perp}\partial_z u\|^2_{L^2(T_{(i+1)})} + \sum_{|\alpha_\perp|=2}\|r_e^{1-a_e}\partial^{\alpha_\perp}u\|^2_{L^2(T_{(i+1)})}). \end{aligned}$$

By (41) and Corollary 3.7, $a_e - 1 \geq -\mu_e^*$, $1 - a_e \geq 1 - \gamma_e$. Therefore,

$$\begin{aligned} E &\leq Ch^2(\|r_e^{-\mu_e^*}\partial_z^2 u\|^2_{L^2(T_{(i+1)})} + \sum_{|\alpha_\perp|=1}\|\partial^{\alpha_\perp}\partial_z u\|^2_{L^2(T_{(i+1)})} + \sum_{|\alpha_\perp|=2}\|r_e^{1-\gamma_e}\partial^{\alpha_\perp} u\|^2_{L^2(T_{(i+1)})}) \\ &\leq Ch^2\|u\|^2_{\mathcal{H}^2_{\vec{\gamma}}(T_{(i+1)})}. \end{aligned} \tag{58}$$

Hence, by (55) – (58), we have completed the proof of (53) in Case I.

Case II: $T_{(i)}$ is a v_e-tetrahedron. Let $T_{(k)} \in \mathcal{T}_k$, $1 \leq k \leq i$, be the v_e-tetrahedron, such that $T_{(i)} \subseteq T_{(k)}$ and $T_{(k)}$ is contained in an e-tetrahedron $T_{(k-1)} \in \mathcal{T}_{k-1}$. Then, using the mapping (51), by (52), for $(x, y, z) \in T_{(i+1)}$ and $(\hat{x}, \hat{y}, \hat{z}) \in \hat{T}_{(i+1)}$, we have

$$\begin{cases} dxdydz = 2^{1-k}\kappa_e^{3i-k-2}d\hat{x}d\hat{y}d\hat{z},\ \partial_{\hat{x}}\hat{v} = (\kappa_e^{i-1}\partial_x - b_1 2^{1-k}\kappa_e^{i-k}\partial_z)v; \\ \partial_{\hat{y}}\hat{v} = (\kappa_e^{i-1}\partial_y - b_2 2^{1-k}\kappa_e^{i-k}\partial_z)v,\ \partial_{\hat{z}}\hat{v} = 2^{1-k}\kappa_e^{i-k}\partial_z v; \\ \partial_x v = (\kappa_e^{1-i}\partial_{\hat{x}} + b_1\kappa_e^{1-i}\partial_{\hat{z}})\hat{v},\ \partial_y v = (\kappa_e^{1-i}\partial_{\hat{y}} + b_2\kappa_e^{1-i}\partial_{\hat{z}})\hat{v},\ \partial_z v = 2^{k-1}\kappa_e^{k-i}\partial_{\hat{z}}\hat{v}. \end{cases} \tag{59}$$

Therefore, by Proposition 5.8, (59), $\kappa_e \leq 1/2$, and the standard interpolation estimate, we have

$$\begin{aligned} \|\partial_x(u - u_I)\|^2_{L^2(T_{(i+1)})} &\leq C2^{1-k}\kappa_e^{i-k}\big(\|\partial_{\hat{x}}(\hat{u} - \hat{u}_I)\|^2_{L^2(\hat{T}_{(i+1)})} + \|\partial_{\hat{z}}(\hat{u} - \hat{u}_I)\|^2_{L^2(\hat{T}_{(i+1)})}\big) \\ &\leq C2^{1-k}\kappa_e^{i-k}2^{2(i-n)}|\hat{u}|^2_{H^2(\hat{T}_{(i+1)})} \\ &\leq C2^{2(i-n)}\sum_{|\alpha_\perp|+\alpha_3=2} 2^{2(1-k)\alpha_3}\kappa_e^{2(i-k)\alpha_3}\kappa_e^{(2i-2)(|\alpha_\perp|-1)}\|\partial^{\alpha_\perp}\partial_z^{\alpha_3}u\|^2_{L^2(T_{(i+1)})} \\ &\leq C2^{2(i-n)}\sum_{|\alpha_\perp|+\alpha_3=2} 2^{-2i\alpha_3}\kappa_e^{2i(|\alpha_\perp|-1)}\|\partial^{\alpha_\perp}\partial_z^{\alpha_3}u\|^2_{L^2(T_{(i+1)})}. \end{aligned} \tag{60}$$

A similar calculation for the derivative with respect to y gives

$$\|\partial_y(u - u_I)\|^2_{L^2(T_{(i+1)})} \leq C2^{2(i-n)}\sum_{|\alpha_\perp|+\alpha_3=2} 2^{-2i\alpha_3}\kappa_e^{2i(|\alpha_\perp|-1)}\|\partial^{\alpha_\perp}\partial_z^{\alpha_3}u\|^2_{L^2(T_{(i+1)})}. \tag{61}$$

In the z-direction, by Proposition 5.8, (59), $\kappa_e \leq 1/2$, and following the calculation in (60),

$$\begin{aligned} \|\partial_z(u - u_I)\|^2_{L^2(T_{(i+1)})} &\leq C(2^{1-k}\kappa_e^{i-k})\kappa_e^{2(i-1)}(2^{k-1}\kappa_e^{k-i})^2\|\partial_{\hat{z}}(\hat{u} - \hat{u}_I)\|^2_{L^2(\hat{T}_{(i+1)})} \\ &\leq C2^{1-k}\kappa_e^{i-k}\big(\|\partial_{\hat{x}}(\hat{u} - \hat{u}_I)\|^2_{L^2(\hat{T}_{(i+1)})} + \|\partial_{\hat{z}}(\hat{u} - \hat{u}_I)\|^2_{L^2(\hat{T}_{(i+1)})}\big) \\ &\leq C2^{2(i-n)}\sum_{|\alpha_\perp|+\alpha_3=2} 2^{-2i\alpha_3}\kappa_e^{2i(|\alpha_\perp|-1)}\|\partial^{\alpha_\perp}\partial_z^{\alpha_3}u\|^2_{L^2(T_{(i+1)})}. \end{aligned} \tag{62}$$

Then, by (60) – (62) and (58), we have obtained (53) for Case II.

Then, we complete the proof by summing up the estimates for all the tetrahedra $T_{(i+1)}$ in $L_{e,i}$. ■

Now, we extend the interpolation error estimate to the whole e-tetrahedron.

Corollary 5.10 *Let $T_{(0)} \in \mathcal{T}_0$ be an e-tetrahedron. For $u \in \mathcal{H}^2_{\vec{\gamma}}(\Omega)$, let u_I be its nodal interpolation on $\mathcal{T}_n$. Then, we have*

$$|u - u_I|_{H^1(T_{(0)})} \leq Ch\|u\|_{\mathcal{H}^2_{\vec{\gamma}}(T_{(0)})},$$

where $h = 2^{-n}$ and C depends on $T_{(0)}$ but not on n.

Proof. By Theorem 5.9, it suffices to show the estimate for any tetrahedron $T_{(n)} \in \mathcal{T}_n$ in the last layer $L_{e,n}$. Since $T_{(n)}$ is either an e- or a v_e-tetrahedron, we derive this estimate in two cases.

Case I: $T_{(n)}$ is an e-tetrahedron. By Proposition 5.8, the mapping $\mathbf{B}_{e,n}$ translates $T_{(n)}$ to the reference tetrahedron $\hat{T}$. Consequently, it maps any point $(x, y, z) \in T_{(n)}$ to $(\hat{x}, \hat{y}, \hat{z}) \in \hat{T}$. For a function v on $T_{(n)}$, we define $\hat{v}$ on $\hat{T}$ by

$$\hat{v}(\hat{x}, \hat{y}, \hat{z}) := v(x, y, z).$$

Now, let χ be a smooth cutoff function on $\hat{T}$ such that $\chi = 0$ in a neighborhood of the edge $\hat{e} := \hat{x}_0\hat{x}_1$ and $= 1$ at every other Lagrange node of $\hat{T}$. Let $r_{\hat{e}}$ be the distance to $\hat{e}$. Let $\hat{u}_I$ be the interpolation of $\hat{u}$ on the reference tetrahedron $\hat{T}$. Since $\chi\hat{u} = 0$ in the neighborhood of $\hat{e}$, $(\chi\hat{u})_I = \hat{u}_I$ and

$$|\chi\hat{u}|^2_{H^2(\hat{T})} \le C(\|r_{\hat{e}}^{a_e-1}\partial_{\hat{z}}^2\hat{u}\|^2_{L^2(\hat{T})} + \sum_{|\alpha_\perp|+\alpha_3\le 2,\ \alpha_3<2} \|r_{\hat{e}}^{|\alpha_\perp|-1}\partial^{\alpha_\perp}\partial_{\hat{z}}^{\alpha_3}\hat{u}\|^2_{L^2(\hat{T})}). \tag{63}$$

Define $\hat{w} := \hat{u} - \chi\hat{u}$. Then, by the usual interpolation error estimate, we have

$$\begin{aligned} |\hat{u} - \hat{u}_I|_{H^1(\hat{T})} &= |\hat{w} + \chi\hat{u} - \hat{u}_I|_{H^1(\hat{T})} \le |\hat{w}|_{H^1(\hat{T})} + |\chi\hat{u} - \hat{u}_I|_{H^1(\hat{T})} \\ &= |\hat{w}|_{H^1(\hat{T})} + |\chi\hat{u} - (\chi\hat{u})_I|_{H^1(\hat{T})} \le C(\|\hat{u}\|_{H^1(\hat{T})} + |\chi\hat{u}|_{H^2(\hat{T})}), \end{aligned} \tag{64}$$

where C depends on, through χ, the nodes on $\hat{T}$. Then, using the scaling argument based on (54), by (64), (63), the relation $r_{\hat{e}}(\hat{x}, \hat{y}, \hat{z}) = \kappa_e^{-n} r_e(x, y, z)$, and (39), we have

$$\begin{aligned} \|\partial_x(u - u_I)\|^2_{L^2(T_{(n)})} &\le C2^{-n}\big(\|\partial_{\hat{x}}(\hat{u} - \hat{u}_I)\|^2_{L^2(\hat{T})} + \|\partial_{\hat{z}}(\hat{u} - \hat{u}_I)\|^2_{L^2(\hat{T})}\big) \\ &\le C2^{-n}(\|r_{\hat{e}}^{a_e-1}\partial_{\hat{z}}^2\hat{u}\|^2_{L^2(\hat{T})} + \sum_{|\alpha_\perp|+\alpha_3\le 2,\ \alpha_3<2} \|r_{\hat{e}}^{|\alpha_\perp|-1}\partial^{\alpha_\perp}\partial_{\hat{z}}^{\alpha_3}\hat{u}\|^2_{L^2(\hat{T})}) \\ &\le C\big(2^{-2n}\|r_e^{a_e-1}\partial_z^2 u\|^2_{L^2(T_{(n)})} + \sum_{|\alpha_\perp|+\alpha_3\le 2,\ \alpha_3<2} 2^{-2n\alpha_3}\|r_e^{|\alpha_\perp|-1}\partial^{\alpha_\perp}\partial_z^{\alpha_3}u\|^2_{L^2(T_{(n)})}\big) \\ &\le C\big(2^{-2n}(\|r_e^{a_e-1}\partial_z^2 u\|^2_{L^2(T_{(n)})} + \sum_{|\alpha_\perp|=1} \|\partial^{\alpha_\perp}\partial_z u\|^2_{L^2(T_{(n)})} \\ &\qquad + \|r_e^{-1}\partial_z u\|^2_{L^2(T_{(n)})}) + \sum_{|\alpha_\perp|\le 2} \|r_e^{|\alpha_\perp|-1}\partial^{\alpha_\perp}u\|^2_{L^2(T_{(n)})}\big) \\ &\le C2^{-2n}\big(\|r_e^{a_e-1}\partial_z^2 u\|^2_{L^2(T_{(n)})} + \sum_{|\alpha_\perp|=1} \|\partial^{\alpha_\perp}\partial_z u\|^2_{L^2(T_{(n)})} \\ &\qquad + \|r_e^{-1}\partial_z u\|^2_{L^2(T_{(n)})} + \sum_{|\alpha_\perp|\le 2} \|r_e^{|\alpha_\perp|-1-a_e}\partial^{\alpha_\perp}u\|^2_{L^2(T_{(n)})}\big). \end{aligned} \tag{65}$$

A similar calculation for the derivative with respect to y gives

$$\begin{aligned} \|\partial_y(u - u_I)\|^2_{L^2(T_{(n)})} &\le C2^{-2n}\big(\|r_e^{a_e-1}\partial_z^2 u\|^2_{L^2(T_{(n)})} + \sum_{|\alpha_\perp|=1} \|\partial^{\alpha_\perp}\partial_z u\|^2_{L^2(T_{(n)})} \\ &\qquad + \|r_e^{-1}\partial_z u\|^2_{L^2(T_{(n)})} + \sum_{|\alpha_\perp|\le 2} \|r_e^{|\alpha_\perp|-1-a_e}\partial^{\alpha_\perp}u\|^2_{L^2(T_{(n)})}\big). \end{aligned} \tag{66}$$

In the z-direction, using (64), (63), (54), (39), and the calculation in (65), we have

$$\begin{aligned}\|\partial_z(u-u_I)\|^2_{L^2(T_{(n)})} &= 2^n\kappa_e^{2n}\|\partial_{\hat z}(\hat u-\hat u_I)\|^2_{L^2(\hat T)}\\ &\le 2^{-n}\big(\|\partial_{\hat x}(\hat u-\hat u_I)\|^2_{L^2(\hat T)}+\|\partial_{\hat z}(\hat u-\hat u_I)\|^2_{L^2(\hat T)}\big)\\ &\le C2^{-2n}\big(\|r_e^{a_e-1}\partial_z^2 u\|^2_{L^2(T_{(n)})}+\sum_{|\alpha_\perp|=1}\|\partial^{\alpha_\perp}\partial_z u\|^2_{L^2(T_{(n)})}\\ &\quad +\|r_e^{-1}\partial_z u\|^2_{L^2(T_{(n)})}+\sum_{|\alpha_\perp|\le 2}\|r_e^{|\alpha_\perp|-1-a_e}\partial^{\alpha_\perp}u\|^2_{L^2(T_{(n)})}\big).\end{aligned}\tag{67}$$

By (41) and Corollary 3.7, $a_e-1\ge-\mu_e^*$ and $a_e\le\gamma_e$. Therefore, by (65) – (67), we have

$$\begin{aligned}|u-u_I|^2_{H^1(T_{(n)})} &\le C2^{-2n}\big(\|r_e^{-\mu_e^*}\partial_z^2 u\|^2_{L^2(T_{(n)})}+\sum_{|\alpha_\perp|=1}\|\partial^{\alpha_\perp}\partial_z u\|^2_{L^2(T_{(n)})}\\ &\quad +\|r_e^{-1}\partial_z u\|^2_{L^2(T_{(n)})}+\sum_{|\alpha_\perp|\le 2}\|r_e^{|\alpha_\perp|-1-\gamma_e}\partial^{\alpha_\perp}u\|^2_{L^2(T_{(n)})}\big)\le Ch^2\|u\|^2_{\mathcal{H}^2_\gamma(T_{(n)})},\end{aligned}\tag{68}$$

which proves the estimate for Case I.

Case II: $T_{(n)}$ is a v_e-tetrahedron. Let $T_{(k)}\in\mathcal{T}_k$, $1\le k\le n$, be the v_e-tetrahedron, such that $T_{(n)}\subseteq T_{(k)}$ and $T_{(k)}$ is contained in an e-tetrahedron $T_{(k-1)}\in\mathcal{T}_{k-1}$. By Proposition 5.8, the mapping $\mathbf{B}_{n,k}$ translates $T_{(n)}$ to a v_e-tetrahedron $\hat T_{(n)}\in\hat{\mathcal{T}}_1$. Thus, $\mathbf{B}_{n,k}$ maps every point $(x,y,z)\in T_{(n)}$ to $(\hat x,\hat y,\hat z)\in\hat T_{(n)}$. As in Case I, for a function v on $T_{(n)}$, we define $\hat v$ on $\hat T_{(n)}$ by

$$\hat v(\hat x,\hat y,\hat z):=v(x,y,z).$$

Now let χ be a smooth cutoff function on $\hat T_{(n)}$ such that $\chi=0$ in a neighborhood of $\hat e:=\hat x_0\hat x_1$ of $\hat T$ and $=1$ at every other Lagrange node of $\hat T_{(n)}$. Recall the distance $r_{\hat e}$ to $\hat e$. Since $\chi\hat u=0$ in the neighborhood of the refined vertex, we have $(\chi\hat u)_I=\hat u_I$ on $\hat T_{(n)}$ and

$$|\chi\hat u|^2_{H^2(\hat T_{(n)})}\le C(\|r_{\hat e}^{a_e-1}\partial_{\hat z}^2\hat u\|^2_{L^2(\hat T_{(n)})}+\sum_{|\alpha_\perp|+\alpha_3\le 2,\ \alpha_3<2}\|r_{\hat e}^{|\alpha_\perp|-1}\partial^{\alpha_\perp}\partial_{\hat z}^{\alpha_3}\hat u\|^2_{L^2(\hat T_{(n)})}).\tag{69}$$

Define $\hat w:=\hat u-\chi\hat u$. Then, by the usual interpolation error estimate, we have

$$\begin{aligned}|\hat u-\hat u_I|_{H^1(\hat T_{(n)})} &= |\hat w+\chi\hat u-\hat u_I|_{H^1(\hat T_{(n)})}\le|\hat w|_{H^1(\hat T_{(n)})}+|\chi\hat u-\hat u_I|_{H^1(\hat T_{(n)})}\\ &= |\hat w|_{H^1(\hat T_{(n)})}+|\chi\hat u-(\chi\hat u)_I|_{H^1(\hat T_{(n)})}\le C(\|\hat u\|_{H^1(\hat T_{(n)})}+|\chi\hat u|_{H^2(\hat T_{(n)})}),\end{aligned}\tag{70}$$

where C depends on, through χ, the nodes in the reference element $\hat{T}_{(n)}$. In $L_{e,n}$, $r_e(x,y,z) = \kappa_e^{n-1} r_{\hat{e}}(\hat{x},\hat{y},\hat{z})$. Therefore, by (59), (70), (69), (39), and $\kappa_e \le 1/2$, we have

$$\begin{aligned}
\|\partial_x(u-u_I)\|^2_{L^2(T_{(n)})} &\le C2^{1-k}\kappa_e^{n-k}\big(\|\partial_{\hat{x}}(\hat{u}-\hat{u}_I)\|^2_{L^2(\hat{T}_{(n)})} + \|\partial_{\hat{z}}(\hat{u}-\hat{u}_I)\|^2_{L^2(\hat{T}_{(n)})}\big)\\
&\le C2^{1-k}\kappa_e^{n-k}(\|r_{\hat{e}}^{a_e-1}\partial_{\hat{z}}^2\hat{u}\|^2_{L^2(\hat{T}_{(n)})} + \sum_{|\alpha_\perp|+\alpha_3\le 2,\ \alpha_3<2} \|r_{\hat{e}}^{|\alpha_\perp|-1}\partial^{\alpha_\perp}\partial_{\hat{z}}^{\alpha_3}\hat{u}\|^2_{L^2(\hat{T}_{(n)})})\\
&\le C\big(2^{2(1-k)}\kappa_e^{2(n-k)}\|r_e^{a_e-1}\partial_z^2 u\|^2_{L^2(T_{(n)})}\\
&\qquad + \sum_{|\alpha_\perp|+\alpha_3\le 2,\ \alpha_3<2} 2^{2(1-k)\alpha_3}\kappa_e^{2(n-k)\alpha_3}\|r_e^{|\alpha_\perp|-1}\partial^{\alpha_\perp}\partial_z^{\alpha_3}u\|^2_{L^2(T_{(n)})}\big)\\
&\le C2^{-2n}\big(\|r_e^{a_e-1}\partial_z^2 u\|^2_{L^2(T_{(n)})} + \sum_{|\alpha_\perp|=1}\|\partial^{\alpha_\perp}\partial_z u\|^2_{L^2(T_{(n)})}\\
&\qquad + \|r_e^{-1}\partial_z u\|^2_{L^2(T_{(n)})} + \sum_{|\alpha_\perp|\le 2}\|r_e^{|\alpha_\perp|-1-a_e}\partial^{\alpha_\perp}u\|^2_{L^2(T_{(n)})}\big). \qquad (71)
\end{aligned}$$

A similar calculation for the derivative with respect to y gives

$$\begin{aligned}
\|\partial_y(u-u_I)\|^2_{L^2(T_{(n)})} &\le C2^{-2n}\big(\|r_e^{a_e-1}\partial_z^2 u\|^2_{L^2(T_{(n)})} + \sum_{|\alpha_\perp|=1}\|\partial^{\alpha_\perp}\partial_z u\|^2_{L^2(T_{(n)})}\\
&\qquad + \|r_e^{-1}\partial_z u\|^2_{L^2(T_{(n)})} + \sum_{|\alpha_\perp|\le 2}\|r_e^{|\alpha_\perp|-1-a_e}\partial^{\alpha_\perp}u\|^2_{L^2(T_{(n)})}\big). \qquad (72)
\end{aligned}$$

In the z-direction, by (59), (70), (69), and the calculation in (71), we have

$$\begin{aligned}
\|\partial_z(u-u_I)\|^2_{L^2(T_{(n)})} &= (2^{1-k}\kappa_e^{n-k})\kappa_e^{2(n-1)}(2^{k-1}\kappa_e^{k-n})^2\|\partial_{\hat{z}}(\hat{u}-\hat{u}_I)\|^2_{L^2(\hat{T}_{(n)})}\\
&\le 2^{1-k}\kappa_e^{n-k}\big(\|\partial_{\hat{x}}(\hat{u}-\hat{u}_I)\|^2_{L^2(\hat{T}_{(n)})} + \|\partial_{\hat{z}}(\hat{u}-\hat{u}_I)\|^2_{L^2(\hat{T}_{(n)})}\big)\\
&\le C2^{-2n}\big(\|r_e^{a_e-1}\partial_z^2 u\|^2_{L^2(T_{(n)})} + \sum_{|\alpha_\perp|=1}\|\partial^{\alpha_\perp}\partial_z u\|^2_{L^2(T_{(n)})}\\
&\qquad + \|r_e^{-1}\partial_z u\|^2_{L^2(T_{(n)})} + \sum_{|\alpha_\perp|\le 2}\|r_e^{|\alpha_\perp|-1-a_e}\partial^{\alpha_\perp}u\|^2_{L^2(T_{(n)})}\big). \qquad (73)
\end{aligned}$$

By (41) and Corollary 3.7, $a_e - 1 \ge -\mu_e^*$ and $a_e \le \gamma_e$. Therefore, by (71) – (73), we have

$$|u-u_I|^2_{H^1(T_{(n)})} \le Ch^2\|u\|^2_{\mathcal{H}^2_{\boldsymbol{\gamma}}(T_{(n)})},$$

which proves the estimate for Case II.

Hence, the corollary is proved by summing up the estimates in Theorem 5.9 and the estimates for all the tetrahedra $T_{(n)}$ in $L_{e,n}$. ■

5.3 Estimates on initial ev-tetrahedra in $\mathcal{T}_0$

In this subsection, we denote by $T_{(0)} = \triangle^4 x_0x_1x_2x_3 \in \mathcal{T}_0$ an ev-tetrahedron, such that $x_0 = c \in \mathcal{C}$ and x_0x_1 is on the edge $e \in \mathcal{E}_c$. Then, we first have mesh layers associated with $\mathcal{T}_n$ on $T_{(0)}$.

Definition 5.11 *(Mesh Layers in ev-tetrahedra) For $1 \le i \le n$, the ith refinement on $T_{(0)}$ produces a small tetrahedron with x_0 as a vertex. We denote by $P_{ev,i}$ the face of this small tetrahedron whose*

closure does not contain x_0 (see the last two pictures in Figure 1). Then, for the mesh $\mathcal{T}_n$ on $T_{(0)}$, we define the ith mesh layer $L_{ev,i}$, $1 \le i < n$, as the region in $T_{(0)}$ between $P_{ev,i}$ and $P_{ev,i+1}$. We define $L_{ev,0}$ to be the region in $T_{(0)}$ between $\triangle^3 x_1x_2x_3$ and $P_{ev,1}$ and let $L_{ev,n} \subset T_{(0)}$ be the small tetrahedron with x_0 as a vertex that is generated in the nth refinement.

Then, we introduce the reference element for the *ev*-tetrahedron.

Definition 5.12 *(The Reference ev-tetrahedron) The reference ev-tetrahedron $\hat{T} = \triangle^4 \hat{x}_0\hat{x}_1\hat{x}_2\hat{x}_3$ of $T_{(0)}$ is defined in the same way as the reference e-tetrahedron in Definition 5.7. Namely, after replacing the e-tetrahedron in Definition 5.7 by the ev-tetrahedron $T_{(0)}$, $\hat{T}$ is obtained as in (49). For $T_{(0)}$, recall the grading parameters κ_c and κ_e associated with x_0 and x_0x_1, respectively. For the reference ev-tetrahedron $\hat{T}$, one graded refinement using the same parameters κ_c, κ_e, and κ_{ec} for $\hat{x}_0$ and $\hat{x}_0\hat{x}_1$ gives rise to a triangulation on $\hat{T}$, which we denote by $\hat{\mathcal{T}}_1$. Define the union of the seven tetrahedra in $\hat{\mathcal{T}}_1$ away from $\hat{x}_0$ to be the mesh layer $\hat{L}$ on $\hat{T}$. Denote by $\hat{\mathcal{L}}$ the initial triangulation of $\hat{L}$ that contains these seven tetrahedra.*

Then, for an *ev*-tetrahedron $T \subset T_{(0)}$ such that $T \in \mathcal{T}_i$, a mapping can be constructed to take it to the reference element $\hat{T}$ (Lemma 4.22 in [23]).

Proposition 5.13 *For an ev-tetrahedron $T := \triangle^4 \gamma_0\gamma_1\gamma_2\gamma_3 \subset T_{(0)}$ in $\mathcal{T}_i$, $0 \le i \le n$, suppose $\gamma_0 = x_0 = c \in \mathcal{C}$ and $\gamma_0\gamma_1 \subset e \in \mathcal{E}_c$. Use a local Cartesian coordinate system, such that $(\gamma_0+\gamma_1)/2$ is the origin, γ_1 is in the positive z-axis, and γ_2 is in the xz-plane. Then, there is a mapping*

$$\mathbf{B}_{ev,i} = \begin{pmatrix} \kappa_{ec}^{-i} & 0 & 0 \\ 0 & \kappa_{ec}^{-i} & 0 \\ b_1\kappa_{ec}^{-i} & b_2\kappa_{ec}^{-i} & \kappa_c^{-i} \end{pmatrix} \tag{74}$$

with $|b_1|, |b_2| \le C_0$, for $C_0 \ge 0$ depending on $T_{(0)}$ but not on i, such that $\mathbf{B}_{ev,i} : T \to \hat{T}$ is a bijection.

Before we proceed with the interpolation error analysis, we first present some useful estimates regarding the relation between the grading parameters in (41) – (42) and the distance function $R_c(x, y, z)$.

Lemma 5.14 *For an ev-tetrahedron $T_{(0)} \in \mathcal{T}_0$, recall the mesh layer $L_{ev,i}$ in Definition 5.11. Then, in the layer $L_{ev,i}$, $1 \le i < n$, the following inequalities hold:*

$$2^i\kappa_{ec}^{ia_e} \lesssim R_c^{a_e-a_{ec}}, \quad 2^i\kappa_c^i \lesssim R_c^{1-a_C}, \quad 2^i\kappa_{ec}^{-ia_e}\kappa_c^{2i} \lesssim R_c^{2-a_C-a_e}. \tag{75}$$

For $(x, y, z) \in L_{ev,n}$, let $(\hat{x}, \hat{y}, \hat{z}) \in \hat{T}$ be its image under $\mathbf{B}_{ev,n}$. Let $R_{\hat{c}}(\hat{x}, \hat{y}, \hat{z})$ be the distance from $(\hat{x}, \hat{y}, \hat{z})$ to $\hat{x}_0$. Then, we have

$$2^n\kappa_{ec}^{na_e} R_{\hat{c}}^{a_e-a_{ec}} \lesssim R_c^{a_e-a_{ec}}, \quad 2^n\kappa_c^n R_{\hat{c}}^{1-a_C} \lesssim R_c^{1-a_C}, \tag{76}$$

$$2^n\kappa_{ec}^{-na_e}\kappa_c^{2n} R_{\hat{c}}^{2-a_C-a_e} \lesssim R_c^{2-a_C-a_e}. \tag{77}$$

Proof. Recall the relations of parameters in (39) and (40). Based on Definition 5.12 and Proposition 5.13, we have $\kappa_{ec}^i \lesssim R_c \lesssim \kappa_c^i$ on $L_{ev,i}$ and

$$\kappa_{ec}^n R_{\hat{c}}(\hat{x}, \hat{y}, \hat{z}) \lesssim R_c(x, y, z) \lesssim \kappa_c^n R_{\hat{c}}(\hat{x}, \hat{y}, \hat{z}) \quad \text{on } L_{ev,n}. \tag{78}$$

Then, since $a_{ec} \le a_e$, on $L_{ev,i}$, we have

$$2^i \kappa_{ec}^{ia_e} = \kappa_{ec}^{i(a_e - a_{ec})} \lesssim R_c^{a_e - a_{ec}};$$

on $L_{ev,n}$, by (78), we have

$$2^n \kappa_{ec}^{na_e} R_{\hat{c}}^{a_e - a_{ec}} = \kappa_{ec}^{n(a_e - a_{ec})} R_{\hat{c}}^{a_e - a_{ec}} \lesssim R_c^{a_e - a_{ec}}.$$

This proves the first inequalities in (75) and (76).

For the second inequalities in (75) and (76), we first note that by (42) and the regularity estimates in Corollary 3.7, we have $a_c \le a_C \le \gamma_c \le 1$. Then, by (42), we have for $1 \le k \le n$,

$$2^k \kappa_c^k = 2^{k - k/a_c} \le 2^{-k/a_{ec} + k a_C / a_{ec}} = \kappa_{ec}^{k(1-a_C)}.$$

Since $1 - a_C \ge 1 - \gamma_c \ge 0$, by (78), we have

$$\begin{aligned} 2^i \kappa_c^i &\le \kappa_{ec}^{i(1-a_C)} \lesssim R_c^{1-a_C} \quad \text{on } L_{ev,i}, \\ 2^n \kappa_c^n R_{\hat{c}}^{1-a_C} &\le \kappa_{ec}^{n(1-a_C)} R_{\hat{c}}^{1-a_C} \lesssim R_c^{1-a_C} \quad \text{on } L_{ev,n}. \end{aligned}$$

Thus, these inequalities are proved.

For the third inequality in (75) and the inequality in (77), by (42) and the regularity estimates in Corollary 3.7, we first have

$$2 - a_C - a_e \ge 2 - \gamma_c - a_e \ge 0.$$

Therefore, by (39), (40), and (42), for $1 \le k \le n$, we have

$$2^k \kappa_{ec}^{-ka_e} \kappa_c^{2k} = 2^k \kappa_{ec}^{-ka_e} \kappa_{ec}^{k(2 - a_C + a_{ec})} = \kappa_{ec}^{k(2 - a_C - a_e)}.$$

Thus, by (78), we have

$$\begin{aligned} 2^i \kappa_{ec}^{-ia_e} \kappa_c^{2i} &= \kappa_{ec}^{i(2 - a_C - a_e)} \lesssim R_c^{2 - a_C - a_e} \quad \text{on } L_{ev,i}, \\ 2^n \kappa_{ec}^{-na_e} \kappa_c^{2n} R_{\hat{c}}^{2 - a_C - a_e} &= \kappa_{ec}^{n(2 - a_C - a_e)} R_{\hat{c}}^{2 - a_C - a_e} \lesssim R_c^{2 - a_C - a_e} \quad \text{on } L_{ev,n}. \end{aligned}$$

Hence, the proof is completed. ■

Now, we formulate the interpolation error estimate on the mesh layers.

Theorem 5.15 *Let $T_{(0)} = \triangle^4 x_0 x_1 x_2 x_3 \in \mathcal{T}_0$ be an ev-tetrahedron defined above. Let $L_{ev,i}$ be the mesh layer in Definition 5.11, $0 \le i < n$. Let u_I be the nodal interpolation of $u \in \mathcal{H}^2_{\boldsymbol{\gamma}}(\Omega)$ on $\mathcal{T}_n$. Then, we have*

$$|u - u_I|^2_{H^1(L_{ev,i})} \le C h^2 \|u\|^2_{\mathcal{H}^2_{\boldsymbol{\gamma}}(L_{ev,i})},$$

where $h = 2^{-n}$ and C depends on $T_{(0)}$ but not on i.

Proof. Let $T_{(i)} \subset T_{(0)}$ be the *ev*-tetrahedron in $\mathcal{T}_i$. Then by Definition 5.11, we have $L_{ev,i} = T_{(i)} \setminus T_{(i+1)}$. Recall the mapping $\mathbf{B}_{ev,i}$ in (74) translates $L_{ev,i}$ to $\hat{L}$ (see Definition 5.12). For a point $(x, y, z) \in L_{ev,i}$, let $(\hat{x}, \hat{y}, \hat{z}) \in \hat{L}$ be its image under $\mathbf{B}_{ev,i}$. For a function v on $L_{ev,i}$, define the function $\hat{v}$ on $\hat{L}$ by

$$\hat{v}(\hat{x}, \hat{y}, \hat{z}) := v(x, y, z).$$

Let $r_{\hat{e}}$ be the distance to $\hat{x}_0\hat{x}_1$ on the reference ev-tetrahedron $\hat{T}$. Then, it is clear that $r_e(x,y,z) = \kappa_{ec}^i r_{\hat{e}}(\hat{x},\hat{y},\hat{z})$ on $L_{ev,i}$. Meanwhile, $\mathbf{B}_{ev,i}$ maps the triangulation $\mathcal{T}_n$ on $L_{ev,i}$ to a graded triangulation on $\hat{L}$ that is obtained after $i+1-n$ refinements of the initial mesh $\hat{\mathcal{L}}$. Note that the subsequent refinements on $\hat{\mathcal{L}}$ are anisotropic with the parameter κ_e toward $\hat{x}_0\hat{x}_1$, since $\hat{\mathcal{L}}$ does not contain ev- or v-tetrahedra. Then, by the mapping (74), the scaling argument, Lemma 5.1, Corollary 5.5, Corollary 5.10, (39), and Lemma 5.14, we have

$$\begin{aligned}
\|\partial_x(u-u_I)\|^2_{L^2(L_{ev,i})} &\leq C\kappa_c^i\big(\|\partial_{\hat{x}}(\hat{u}-\hat{u}_I)\|^2_{L^2(\hat{L})} + \|\partial_{\hat{z}}(\hat{u}-\hat{u}_I)\|^2_{L^2(\hat{L})}\big)\\
&\leq C\kappa_c^i 2^{2(i-n)}\big(\|r_{\hat{e}}^{a_e-1}\partial_{\hat{z}}^2\hat{u}\|^2_{L^2(\hat{L})} + \sum_{|\alpha_\perp|=1}\|\partial^{\alpha_\perp}\partial_{\hat{z}}\hat{u}\|^2_{L^2(\hat{L})}\\
&\qquad + \|r_{\hat{e}}^{-1}\partial_{\hat{z}}\hat{u}\|^2_{L^2(\hat{L})} + \sum_{|\alpha_\perp|\leq 2}\|r_{\hat{e}}^{|\alpha_\perp|-1-a_e}\partial^{\alpha_\perp}\hat{u}\|^2_{L^2(\hat{L})}\big)\\
&\leq C2^{-2n}\big(2^{2i}\kappa_c^{4i}\kappa_{ec}^{-2ia_e}\|r_e^{a_e-1}\partial_z^2 u\|^2_{L^2(L_{ev,i})} + 2^{2i}\kappa_c^{2i}\sum_{|\alpha_\perp|=1}\|\partial^{\alpha_\perp}\partial_z u\|^2_{L^2(L_{ev,i})}\\
&\qquad + 2^{2i}\kappa_c^{2i}\|r_e^{-1}\partial_z u\|^2_{L^2(L_{ev,i})} + 2^{2i}\kappa_{ec}^{2ia_e}\sum_{|\alpha_\perp|\leq 2}\|r_e^{|\alpha_\perp|-1-a_e}\partial^{\alpha_\perp}u\|^2_{L^2(L_{ev,i})}\big)\\
&\leq C2^{-2n}\big(\|R_c^{2-a_C-a_e}r_e^{a_e-1}\partial_z^2 u\|^2_{L^2(L_{ev,i})} + \sum_{|\alpha_\perp|=1}\|R_c^{1-a_C}\partial^{\alpha_\perp}\partial_z u\|^2_{L^2(L_{ev,i})}\\
&\qquad + \|R_c^{1-a_C}r_e^{-1}\partial_z u\|^2_{L^2(L_{ev,i})} + \sum_{|\alpha_\perp|\leq 2}\|R_c^{a_e-a_{ec}}r_e^{|\alpha_\perp|-1-a_e}\partial^{\alpha_\perp}u\|^2_{L^2(L_{ev,i})}\big).
\end{aligned}$$

Note that the estimates in Lemma 5.14 were used to obtain the last inequality above (from different factors involving κ_c, κ_{ec} to factors in terms of R_c). Recall $\theta_{c,e} = r_e/R_c$. By (41) and (42), we have $a_e \leq \gamma_e$, $-\mu_e^* \leq a_e - 1 \leq 0$, and $a_{ec} \leq a_C \leq \gamma_c$. Therefore,

$$\begin{aligned}
\|\partial_x(u-u_I)\|^2_{L^2(L_{ev,i})} &\leq Ch^2\big(\|R_c^{1-a_C}\theta_{c,e}^{a_e-1}\partial_z^2 u\|^2_{L^2(L_{ev,i})} + \sum_{|\alpha_\perp|=1}\|R_c^{1-a_C}\partial^{\alpha_\perp}\partial_z u\|^2_{L^2(L_{ev,i})}\\
&\quad + \|R_c^{-a_C}\theta_{c,e}^{-1}\partial_z u\|^2_{L^2(L_{ev,i})} + \sum_{|\alpha_\perp|\leq 2}\|R_c^{|\alpha_\perp|-1-a_{ec}}\theta_{c,e}^{|\alpha_\perp|-1-a_e}\partial^{\alpha_\perp}u\|^2_{L^2(L_{ev,i})}\big)\\
&\leq Ch^2\big(\|R_c^{1-\gamma_c}\theta_{c,e}^{-\mu_e^*}\partial_z^2 u\|^2_{L^2(L_{ev,i})} + \sum_{|\alpha_\perp|=1}\|R_c^{1-\gamma_c}\partial^{\alpha_\perp}\partial_z u\|^2_{L^2(L_{ev,i})}\\
&\quad + \|R_c^{-\gamma_c}\theta_{c,e}^{-1}\partial_z u\|^2_{L^2(L_{ev,i})} + \sum_{|\alpha_\perp|\leq 2}\|R_c^{|\alpha_\perp|-1-\gamma_c}\theta_{c,e}^{|\alpha_\perp|-1-\gamma_e}\partial^{\alpha_\perp}u\|^2_{L^2(L_{ev,i})}\big)\\
&\leq Ch^2\|u\|^2_{\mathcal{H}^2_{\boldsymbol{\gamma}}(L_{ev,i})}. \qquad (79)
\end{aligned}$$

In the y-direction, with a similar process, we obtain

$$\|\partial_y(u-u_I)\|^2_{L^2(L_{ev,i})} \leq Ch^2\|u\|^2_{\mathcal{H}^2_{\boldsymbol{\gamma}}(L_{ev,i})}. \qquad (80)$$

In the z-direction, by the mapping (74), the scaling argument, $\kappa_{ec} \leq \kappa_c$, and the calculation above,

$$\begin{aligned}
\|\partial_z(u-u_I)\|^2_{L^2(L_{ev,i})} &= \kappa_c^{-i}\kappa_{ec}^{2i}\|\partial_{\hat{z}}(\hat{u}-\hat{u}_I)\|^2_{L^2(\hat{L})}\\
&\leq C\kappa_c^i\big(\|\partial_{\hat{x}}(\hat{u}-\hat{u}_I)\|^2_{L^2(\hat{L})} + \|\partial_{\hat{z}}(\hat{u}-\hat{u}_I)\|^2_{L^2(\hat{L})}\big)\\
&\leq Ch^2\|u\|^2_{\mathcal{H}^2_{\boldsymbol{\gamma}}(L_{ev,i})}. \qquad (81)
\end{aligned}$$

Hence, the proof is completed by the estimates in (79) – (81). ∎

Then, we are ready to obtain the interpolation error estimate on the whole *ev*-tetrahedron $T_{(0)}$.

Corollary 5.16 *Let $T_{(0)} \in \mathcal{T}_0$ be an ev-tetrahedron as in Theorem 5.15. Let u_I be the nodal interpolation of $u \in \mathcal{H}^2_{\boldsymbol{\gamma}}(\Omega)$ on $\mathcal{T}_n$. Then, we have*

$$|u - u_I|^2_{H^1(T_{(0)})} \le Ch\|u\|^2_{\mathcal{H}^2_{\boldsymbol{\gamma}}(T_{(0)})},$$

where $h = 2^{-n}$ and C depends on $T_{(0)}$ but not on n.

Proof. By Theorem 5.15, it suffices to show for the last layer $L_{ev,n}$

$$|u - u_I|^2_{H^1(L_{ev,n})} \le Ch^2\|u\|^2_{\mathcal{H}^2_{\boldsymbol{\gamma}}(L_{ev,n})}.$$

By Proposition 5.13, $\mathbf{B}_{ev,n}(L_{ev,n}) = \hat{T}$. For $(x,y,z) \in L_{ev,n}$, let $(\hat{x},\hat{y},\hat{z}) \in \hat{T}$ be its image under $\mathbf{B}_{ev,n}$. For a function v on $L_{ev,n}$, we define $\hat{v}$ on $\hat{T}$ by

$$\hat{v}(\hat{x},\hat{y},\hat{z}) := v(x,y,z).$$

Now, let χ be a smooth cutoff function on $\hat{T}$ such that $\chi = 0$ in a neighborhood of the edge $\hat{e} := \hat{x}_0\hat{x}_1$ and $= 1$ at every other node of $\hat{T}$. Let $R_{\hat{c}}$ (resp. $r_{\hat{e}}$) be the distance from $(\hat{x},\hat{y},\hat{z})$ to $\hat{x}_0$ (resp. $\hat{e}$). Then, by (74), $\kappa^n_{ec} r_{\hat{e}}(\hat{x},\hat{y},\hat{z}) = r_e(x,y,z)$. Let $\hat{u}_I$ be the interpolation of $\hat{u}$ on the reference tetrahedron $\hat{T}$. Since $\chi\hat{u} = 0$ in the neighborhood of $\hat{e}$, $(\chi\hat{u})_I = \hat{u}_I$ and

$$\begin{aligned} |\chi\hat{u}|^2_{H^2(\hat{T})} \;\le\; & C\big(\|R^{2-a_C-a_e}_{\hat{c}} r^{a_e-1}_{\hat{e}} \partial^2_{\hat{z}}\hat{u}\|^2_{L^2(\hat{T})} + \sum_{|\alpha_\perp|=1} \|R^{1-a_C}_{\hat{c}} \partial^{\alpha_\perp}\partial_{\hat{z}}\hat{u}\|^2_{L^2(\hat{T})} \\ & + \|R^{1-a_C}_{\hat{c}} r^{-1}_{\hat{e}} \partial_{\hat{z}}\hat{u}\|^2_{L^2(\hat{T})} + \sum_{|\alpha_\perp|\le 2} \|R^{a_e-a_{ec}}_{\hat{c}} r^{|\alpha_\perp|-1-a_e}_{\hat{e}} \partial^{\alpha_\perp}\hat{u}\|^2_{L^2(\hat{T})}\big). \end{aligned} \tag{82}$$

Define $\hat{w} := \hat{u} - \chi\hat{u}$. Then, by the usual interpolation error estimate, $r_{\hat{e}} \lesssim R_{\hat{c}}$, and (82), we have

$$\begin{aligned} |\hat{u} - \hat{u}_I|_{H^1(\hat{T})} &= |\hat{w} + \chi\hat{u} - \hat{u}_I|_{H^1(\hat{T})} \le |\hat{w}|_{H^1(\hat{T})} + |\chi\hat{u} - \hat{u}_I|_{H^1(\hat{T})} \\ &= |\hat{w}|_{H^1(\hat{T})} + |\chi\hat{u} - (\chi\hat{u})_I|_{H^1(\hat{T})} \le C(\|\hat{u}\|_{H^1(\hat{T})} + |\chi\hat{u}|_{H^2(\hat{T})}) \\ &\le C\big(\|R^{2-a_C-a_e}_{\hat{c}} r^{a_e-1}_{\hat{e}} \partial^2_{\hat{z}}\hat{u}\|^2_{L^2(\hat{T})} + \sum_{|\alpha_\perp|=1} \|R^{1-a_C}_{\hat{c}} \partial^{\alpha_\perp}\partial_{\hat{z}}\hat{u}\|^2_{L^2(\hat{T})} \\ &\quad + \|R^{1-a_C}_{\hat{c}} r^{-1}_{\hat{e}} \partial_{\hat{z}}\hat{u}\|^2_{L^2(\hat{T})} + \sum_{|\alpha_\perp|\le 2} \|R^{a_e-a_{ec}}_{\hat{c}} r^{|\alpha_\perp|-1-a_e}_{\hat{e}} \partial^{\alpha_\perp}\hat{u}\|^2_{L^2(\hat{T})}\big), \end{aligned} \tag{83}$$

where C depends on, through χ, the nodes on $\hat{T}$. Then, using (83), the scaling argument based on (74), the relation $r_{\hat{e}}(\hat{x},\hat{y},\hat{z}) = \kappa_{ec}^{-n} r_e(x,y,z)$, and the estimates in (76) and (77), we have

$$\begin{aligned}
\|\partial_x(u-u_I)\|^2_{L^2(L_{ev,n})} &\leq C\kappa_c^n\big(\|\partial_{\hat{x}}(\hat{u}-\hat{u}_I)\|^2_{L^2(\hat{T})} + \|\partial_{\hat{z}}(\hat{u}-\hat{u}_I)\|^2_{L^2(\hat{T})}\big)\\
&\leq C\kappa_c^n\big(\|R_{\hat{c}}^{2-a_C-a_e} r_{\hat{e}}^{a_e-1}\partial_{\hat{z}}^2\hat{u}\|^2_{L^2(\hat{T})} + \sum_{|\alpha_\perp|=1}\|R_{\hat{c}}^{1-a_C}\partial^{\alpha_\perp}\partial_{\hat{z}}\hat{u}\|^2_{L^2(\hat{T})}\\
&\quad + \|R_{\hat{c}}^{1-a_C} r_{\hat{e}}^{-1}\partial_{\hat{z}}\hat{u}\|^2_{L^2(\hat{T})} + \sum_{|\alpha_\perp|\leq 2}\|R_{\hat{c}}^{a_e-a_{ec}} r_{\hat{e}}^{|\alpha_\perp|-1-a_e}\partial^{\alpha_\perp}\hat{u}\|^2_{L^2(\hat{T})}\big)\\
&\leq C\kappa_{ec}^{-2n}\big(\kappa_c^{4n}\|R_{\hat{c}}^{2-a_C-a_e} r_{\hat{e}}^{a_e-1}\partial_z^2 u\|^2_{L^2(L_{ev,n})} + \kappa_{ec}^{2n}\kappa_c^{2n}\sum_{|\alpha_\perp|=1}\|R_{\hat{c}}^{1-a_C}\partial^{\alpha_\perp}\partial_z u\|^2_{L^2(L_{ev,n})}\\
&\quad + \kappa_c^{2n}\|R_{\hat{c}}^{1-a_C} r_{\hat{e}}^{-1}\partial_z u\|^2_{L^2(L_{ev,n})} + \sum_{|\alpha_\perp|\leq 2}\kappa_{ec}^{2n|\alpha_\perp|}\|R_{\hat{c}}^{a_e-a_{ec}} r_{\hat{e}}^{|\alpha_\perp|-1-a_e}\partial^{\alpha_\perp}\hat{u}\|^2_{L^2(L_{ev,n})}\big)\\
&= C2^{-2n}\big(2^{2n}\kappa_{ec}^{-2na_e}\kappa_c^{4n}\|R_{\hat{c}}^{2-a_C-a_e} r_e^{a_e-1}\partial_z^2 u\|^2_{L^2(L_{ev,n})} + 2^{2n}\kappa_c^{2n}\sum_{|\alpha_\perp|=1}\|R_{\hat{c}}^{1-a_C}\partial^{\alpha_\perp}\partial_z u\|^2_{L^2(L_{ev,n})}\\
&\quad + 2^{2n}\kappa_c^{2n}\|R_{\hat{c}}^{1-a_C} r_e^{-1}\partial_z u\|^2_{L^2(L_{ev,n})} + \sum_{|\alpha_\perp|\leq 2} 2^{2n}\kappa_{ec}^{2na_e}\|R_{\hat{c}}^{a_e-a_{ec}} r_e^{|\alpha_\perp|-1-a_e}\partial^{\alpha_\perp}u\|^2_{L^2(L_{ev,n})}\big)\\
&\leq C2^{-2n}\big(\|R_c^{2-a_C-a_e} r_e^{a_e-1}\partial_z^2 u\|^2_{L^2(L_{ev,n})} + \sum_{|\alpha_\perp|=1}\|R_c^{1-a_C}\partial^{\alpha_\perp}\partial_z u\|^2_{L^2(L_{ev,n})}\\
&\quad + \|R_c^{1-a_C} r_e^{-1}\partial_z u\|^2_{L^2(L_{ev,n})} + \sum_{|\alpha_\perp|\leq 2}\|R_c^{a_e-a_{ec}} r_e^{|\alpha_\perp|-1-a_e}\partial^{\alpha_\perp}u\|^2_{L^2(L_{ev,n})}\big).
\end{aligned}$$

By (41) and (42), we have $a_e \leq \gamma_e$, $-\mu_e^* \leq a_e - 1 \leq 0$ and $a_{ec} \leq a_C \leq \gamma_c$. Therefore,

$$\begin{aligned}
\|\partial_x(u-u_I)\|^2_{L^2(L_{ev,n})} &\leq Ch^2\big(\|R_c^{1-a_C}\theta_{c,e}^{a_e-1}\partial_z^2 u\|^2_{L^2(L_{ev,n})} + \sum_{|\alpha_\perp|=1}\|R_c^{1-a_C}\partial^{\alpha_\perp}\partial_z u\|^2_{L^2(L_{ev,n})}\\
&\quad + \|R_c^{-a_C}\theta_{c,e}^{-1}\partial_z u\|^2_{L^2(L_{ev,n})} + \sum_{|\alpha_\perp|\leq 2}\|R_c^{|\alpha_\perp|-1-a_{ec}}\theta_{c,e}^{|\alpha_\perp|-1-a_e}\partial^{\alpha_\perp}u\|^2_{L^2(L_{ev,n})}\big)\\
&\leq Ch^2\big(\|R_c^{1-\gamma_c}\theta_{c,e}^{-\mu_e^*}\partial_z^2 u\|^2_{L^2(L_{ev,n})} + \sum_{|\alpha_\perp|=1}\|R_c^{1-\gamma_c}\partial^{\alpha_\perp}\partial_z u\|^2_{L^2(L_{ev,n})}\\
&\quad + \|R_c^{-\gamma_c}\theta_{c,e}^{-1}\partial_z u\|^2_{L^2(L_{ev,n})} + \sum_{|\alpha_\perp|\leq 2}\|R_c^{|\alpha_\perp|-1-\gamma_c}\theta_{c,e}^{|\alpha_\perp|-1-\gamma_e}\partial^{\alpha_\perp}u\|^2_{L^2(L_{ev,n})}\big)\\
&\leq Ch^2\|u\|^2_{\mathcal{H}^2_{\vec{\gamma}}(L_{ev,n})}. \qquad (84)
\end{aligned}$$

A similar error estimate in the y-direction leads to

$$\|\partial_y(u-u_I)\|^2_{L^2(L_{ev,n})} \leq Ch^2\|u\|^2_{\mathcal{H}^2_{\vec{\gamma}}(L_{ev,n})}. \qquad (85)$$

In the z-direction, using $\kappa_c \geq \kappa_{ec}$, the scaling argument based on (74), and the calculation above for $\|\partial_x(u-u_I)\|_{L^2(L_{ev,n})}$, we have

$$\begin{aligned}
\|\partial_z(u-u_I)\|^2_{L^2(L_{ev,n})} &= \kappa_c^{-n}\kappa_{ec}^{2n}\|\partial_{\hat{z}}(\hat{u}-\hat{u}_I)\|^2_{L^2(\hat{T})}\\
&\leq \kappa_c^n\big(\|\partial_{\hat{x}}(\hat{u}-\hat{u}_I)\|^2_{L^2(\hat{T})} + \|\partial_{\hat{z}}(\hat{u}-\hat{u}_I)\|^2_{L^2(\hat{T})}\big)\\
&\leq Ch^2\|u\|^2_{\mathcal{H}^2_{\vec{\gamma}}(L_{ev,n})}. \qquad (86)
\end{aligned}$$

Thus, the proof is completed by (84) – (86). ■

Based on the interpolation error estimates in this section, we therefore obtain our main result on the convergence rate for the anisotropic FEM.

Theorem 5.17 *Under the assumption in Lemma 3.2, for $f \in L_{\boldsymbol{\mu}^*}(\Omega)$ defined in (10), the proposed finite element approximation (Algorithm 4.4) of equation (1) achieves the optimal rate of convergence. Namely,*

$$|u - u_n|_{H^1(\Omega)} \leq C \dim(S_n)^{-1/3} \|f\|_{L^2_{\boldsymbol{\mu}^*}(\Omega)},$$

where $dim(S_n)$ is the dimension of the finite element space associated with $\mathcal{T}_n$, and the constant C depends on $\mathcal{T}_0$, but not on n.

Proof. Recall the local interpolation error estimates on different initial tetrahedra: the o-tetrahedra (Lemma 5.1), the v- or v_e-tetrahedra (Corollary 5.5), the e-tetrahedra (Corollary 5.10), and the ev-tetrahedra (Corollary 5.16). Then, based on (4) and the regularity estimates in Corollary 3.7, for $h = 2^{-n}$, we have

$$|u - u_n|_{H^1(\Omega)} \leq |u - u_I|_{H^1(\Omega)} \leq Ch\|u\|_{\mathcal{H}^2_{\boldsymbol{\gamma}}(\Omega)} \leq Ch\|f\|_{L^2_{\boldsymbol{\mu}^*}(\Omega)}.$$

Note that in a refinement, each tetrahedron is decomposed into 8 sub-tetrahedra. Therefore, the dimension of the finite element space $\dim(S_n) \sim 2^{3n}$. Thus, the result follows from $h \sim \dim(S_n)^{-1/3}$. ■

6 Numerical results

In this section, we use Algorithm 4.4 to solve equation (1) with the given data f in the weighted L^2 space. The numerical tests are implemented on two polyhedral domains that give rise to typical three dimensional edge and vertex-edge solution singularities: the prism and the Fichera corner. It will be evident that the numerical results are aligned with our approximation results presented in Section 4 and Section 5, and thus validate our method.

6.1 Test I (The Prism Domain)

Let T be the triangle with vertices $(0,0), (1,0)$, and $(0.5, 0.5)$, and let the domain be the prism $\Omega := \big((0,1)^2 \setminus T\big) \times (0,1)$ (Figure 4). Note that the edge e with the opening angle $\omega_e = 3\pi/2$ is the only singular edge. We solve equation (1) with $f = |z - 0.5|^{0.1}$ using Algorithm 4.4. It is clear that $f \notin H^1(\Omega)$ but $f \in L^2_{\boldsymbol{\mu}^*}(\Omega)$ for any

$$1/2 \leq \mu_e^* < \pi/\omega_e = 2/3. \tag{87}$$

Based on the regularity estimates in Corollary 3.7, the solution is in H^2 in the sub-region of Ω that is away from the edge e. Then, a quasi-uniform mesh in such a region will yield a first-order (optimal) convergence for the interpolation error. Meanwhile, according to Algorithm 4.4, the condition (87) leads to the optimal range of the parameter

$$1/3 \leq a_e < 2/3, \quad \text{namely, } 0.125 \leq \kappa_e = 2^{-1/a_e} < 0.353. \tag{88}$$

In a sufficiently small neighborhood $\mathcal{V}$ of the endpoints c of e, using the notation in [10], by Table 1 in [14], we have $f \in M^2_{\boldsymbol{\beta}-1}(\mathcal{V})$, for $0 < \beta_e < 2/3$ and $0 < \beta_c < 13/6$, and therefore $u \in M^2_{\boldsymbol{\beta}+1}(\mathcal{V}')$,

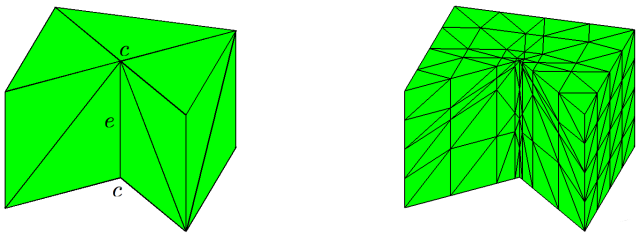

Figure 4: The prism domain: the initial triangulation (left) and the mesh after two graded refinements toward the singular edge e ($\kappa_e = 0.2$).

j	$\kappa_e = 0.2$	$\kappa_e = 0.3$	$\kappa_e = 0.4$	$\kappa_e = 0.5$
3	0.77	0.81	0.83	0.82
4	0.92	0.93	0.93	0.90
5	0.97	0.98	0.96	0.91
6	0.99	0.99	0.97	0.89

Table 1: Convergence rates in the H^1 norm for the prism domain with different edge refinements ($\kappa_c = 0.5$).

for a smaller neighborhood $\mathcal{V}'$ of these endpoints. This implies that for any $a_c, a_e \in (0, 1]$, these vertices shall not affect the convergence rate of the numerical solution. See [23] for the detailed argument. Therefore, to achieve the optimal convergence rate, it is sufficient to only implement special edge refinement based on the value of κ_e in (88).

Thus, in the numerical tests, we fix the parameter $\kappa_c = 0.5$ ($a_c = 1$) for either of the vertices c in order to verify the optimal range for the edge parameter κ_e. Recall that for $\kappa_{ec} = \kappa_e < 0.5$ and $\kappa_c = 0.5$, the resulting mesh is graded toward the edge e without special refinement for the vertex c. See Figure 4 for such graded meshes when $\kappa_e = 0.2$.

In Table 1, we display the convergence rates of the finite element solution on proposed anisotropic meshes associated with different values of the grading parameter κ_e. Here, j is the level of refinements. Denote by u_j the linear finite element solution on the mesh after j refinements. Since the exact solution is not known, the convergence rate is computed using the numerical solutions for successive mesh refinements

$$\text{convergence rate} = \log_2\left(\frac{|u_j - u_{j-1}|_{H^1(\Omega)}}{|u_{j+1} - u_j|_{H^1(\Omega)}}\right). \tag{89}$$

As j increases, the dimension of the discrete system is $O(2^{3j})$. Therefore, the asymptotic convergence rate in (89) is a reasonable indicator of the actual convergence rate for the numerical solution. See the Appendix for a brief illustration on the validation of (89).

It is clear from Table 1 that the first-order convergence rate is obtained for $0.125 \le \kappa_e = 0.2, 0.3 < 0.353$, while we lose the optimal convergence rate if $\kappa_e = 0.4, 0.5$, both larger than the critical value 0.353. When $\kappa_e = 0.4$, that is $0.353 < \kappa_e < 0.5$, this choice still leads to an anisotropic mesh graded toward the singular edge, but the grading is insufficient to resolve the edge singularity in the solution, and hence does not lead to the optimal rate of convergence. These results are in agreement with the sufficient condition (88) for the optimal convergence rate in Algorithm 4.4.

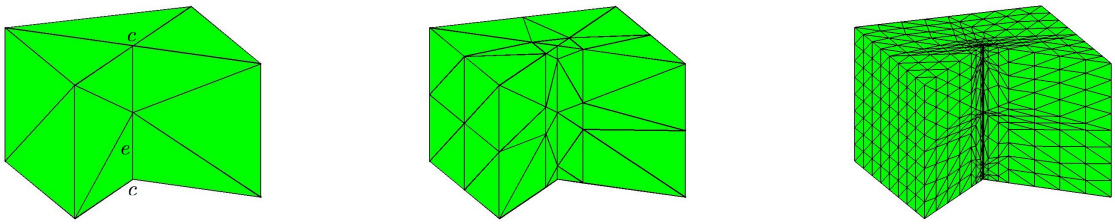

Figure 5: The prism domain (left – right): the initial mesh, mesh after one refinement, mesh after three refinements ($\kappa_e = \kappa_c = 0.2$).

j	$\kappa = 0.2$	$\kappa = 0.3$	$\kappa = 0.4$	$\kappa = 0.5$
3	0.82	0.84	0.85	0.83
4	0.94	0.94	0.93	0.88
5	0.98	0.98	0.96	0.88
6	0.99	0.99	0.96	0.86

Table 2: Convergence rates in the H^1 norm for the prism domain with edge and vertex refinements ($\kappa := \kappa_e = \kappa_c$).

Besides the edge refinements in Table 1 ($\kappa_c = 0.5$), we list additional numerical test results in Table 2, where we choose $\kappa_c = \kappa_e$ for the endpoints c of the singular edge e. See Figure 5 for an example of the mesh. Note that based on the argument above and on (88), the optimal convergence rate only depends on the edge parameter κ_e for the prism domain. This can be clearly seen from the similar convergence results in Table 2. Namely, optimal convergence rates are achieved when κ_e is in the range given by (88). We report these results to illustrate the flexibility of our meshing options in the proposed algorithm.

6.2 Test II (The Fichera Corner)

Define the two cubes: $D_0 = (0,1)^3$ and $D_1 = [0.5,1) \times (0,0.5] \times [0.5,1)$. Let the $\Omega := D_0 \setminus D_1$. Thus, the domain Ω is featured with the Fichera corner at the vertex c and three adjacent edges e with the opening angle $3\pi/2$ (Figure 6). Then, the singular edges are the three edges e joining at the Fichera corner c. In this test, we set for equation (1)

$$f = \begin{cases} 0 & \text{in } \Omega_0 := (0,0.5) \times (0.5,1) \times (0,0.5), \\ |x-0.75|^{0.1} + |y-0.25|^{0.1} + |z-0.75|^{0.1} & \text{in } \Omega \setminus \Omega_0. \end{cases}$$

It is clear that $f \notin H^1(\Omega)$ and $f \in L^2_{\boldsymbol{\mu}^*}(\Omega)$ for any $1/2 \le \mu_e^* < 2/3$ for the singular edges.

For a sub-region $\mathcal{D}$ away from these three edges, the solution of equation (1) belongs to $H^2(\mathcal{D})$, and therefore, a quasi-uniform mesh will lead to the optimal convergence rate for the interpolation error. In a sufficiently small neighborhood $\mathcal{V}$ of the endpoints of the three edges that are not at the Fichera corner, following a similar argument as in Test I, $u \in M^2_{\boldsymbol{\beta}+1}(\mathcal{V})$ for $0 < \beta_e < 2/3$ and $0 < \beta_c < 13/6$, and therefore these vertices shall not affect the conference rate for any feasible parameters $a_e, a_c \in (0,1]$. In the neighborhood of the Fichera corner c, by Corollary 3.7 and Table

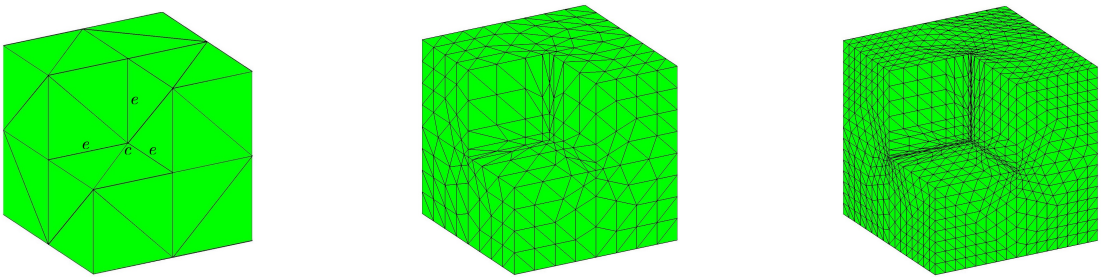

Figure 6: The Fichera corner (left – right): the initial mesh, mesh after two refinements, mesh after three refinements ($\kappa_e = \kappa_c = 0.3$).

j	$\kappa_c = 0.3 \quad \kappa_e = 0.3$	$\kappa_c = 0.5 \quad \kappa_e = 0.5$
3	0.83	0.81
4	0.93	0.87
5	0.97	0.87
6	0.99	0.84

Table 3: Convergence rates in the H^1 norm for the Fichera corner.

1 in [14], the solution satisfies

$$u \in \mathcal{H}^2_{\boldsymbol{\gamma}} \quad \text{for } \mu^*_e \le \gamma_e < \lambda_e = 2/3 \text{ and } \gamma_c < \lambda_c + 1/2 \approx 0.954.$$

Then, by Algorithm 4.4, the sufficient condition to attain the optimal convergence rate for the finite element solution is that the mesh parameters give rise to

$$1/3 \le a_e < 2/3 \text{ (for the three singular edges)} \quad \text{and} \quad a_C < 0.954 \text{ (for the Fichera corner).} \tag{90}$$

There are many possible values of a_e and a_c that fulfill this requirement. To illustrate our method, in Table 3, we list the convergence rates of the finite element solutions on anisotropic meshes with $a_e = a_c = 0.576$ (accordingly, $\kappa_e = \kappa_c = 0.3$) and on quasi-uniform meshes $a_e = a_c = 1$ (accordingly, $\kappa_e = \kappa_c = 0.5$). The rates are computed using numerical solutions as in (89).

In the case $\kappa_e = \kappa_c = 0.3$, by (39) and (42), we have $1/3 \le a_e = 0.576 < 2/3$ and $a_C = a_c = 0.576 < 0.954$. Therefore, by Algorithm 4.4 and Theorem 5.17, we expect to obtain the first-order optimal convergence rate in the finite element approximation. As for the quasi-uniform mesh ($\kappa_e = \kappa_c = 0.5$), since the solution is not globally in H^2, by (5), we expect a sub-optimal convergence rate. It is clear that the numerical results in Table 3 validate this theoretical prediction and hence verify Algorithm 4.4.

6.3 The L^2 convergence

We end this section by including the convergence rates of the numerical solutions in the L^2 norm on the same graded meshes given in Table 1 ($\kappa_c = 0.5$) for the prism domain and in Table 3 for the domain with the Fichera corner. These results are displayed in Table 4 and in Table 5, respectively.

We see that for the prism domain, the second-order (optimal) L^2 convergence rates are obtained for $\kappa_e = 0.2$ and 0.3; while the convergence slows down otherwise. For the domain with the Fichera

j	$\kappa_e = 0.2$	$\kappa_e = 0.3$	$\kappa_e = 0.4$	$\kappa_e = 0.5$
3	1.62	1.69	1.72	1.69
4	1.88	1.90	1.88	1.78
5	1.96	1.96	1.93	1.75
6	1.99	1.99	1.94	1.66

Table 4: Convergence rates in the L^2 norm for the prism domain with different edge refinements ($\kappa_c = 0.5$).

j	$\kappa_c = 0.3 \quad \kappa_e = 0.3$	$\kappa_c = 0.5 \quad \kappa_e = 0.5$
3	1.71	1.63
4	1.87	1.66
5	1.95	1.60
6	1.98	1.52

Table 5: Convergence rates in the L^2 norm for the Fichera corner.

corner, the L^2 convergence is optimal when $\kappa_c = \kappa_e = 0.3$, which is apparently better than that on the quasi-uniform mesh ($\kappa_c = \kappa_e = 0.5$). This is consistent with the H^1 convergence rates in Table 1 and in Table 3. Let us point out that it is probably possible to derive the L^2 error analysis on the proposed anisotropic meshes using a duality argument. This is outside the scope of this paper and will be investigated in the future.

7 Appendix

We here illustrate that the numerical convergence rate in (89) is a reasonable indicator for the actual convergence rate. Assume

$$|u - u_j|_{H^1(\Omega)} = C2^{-sj},$$

where $0 < s \leq 1$ is the convergence rate and $C > 0$ is independent of j. Recall the Galerkin orthogonality

$$a(u, u_j) = a(u_j, u_j) \quad \text{and} \quad a(u - u_{j-1}, u_{j-1}) = a(u_j - u_{j-1}, u_{j-1}) = 0.$$

Then,

$$|u - u_j|^2_{H^1(\Omega)} = a(u - u_j, u - u_j) = a(u - u_j, u) = a(u, u) - a(u_j, u_j) = |u|^2_{H^1(\Omega)} - |u_j|^2_{H^1(\Omega)},$$

and

$$\begin{aligned} |u_j - u_{j-1}|^2_{H^1(\Omega)} &= a(u_j - u_{j-1}, u_j - u_{j-1}) = a(u_j - u_{j-1}, u_j) \\ &= a(u_j, u_j) - a(u_{j-1}, u_{j-1}) = |u_j|^2_{H^1(\Omega)} - |u_{j-1}|^2_{H^1(\Omega)}. \end{aligned}$$

Therefore, we have

$$\begin{aligned} |u_j - u_{j-1}|^2_{H^1(\Omega)} &= |u_j|^2_{H^1(\Omega)} - |u_{j-1}|^2_{H^1(\Omega)} = |u|^2_{H^1(\Omega)} - |u_{j-1}|^2_{H^1(\Omega)} - (|u|^2_{H^1(\Omega)} - |u_j|^2_{H^1(\Omega)}) \\ &= |u - u_{j-1}|^2_{H^1(\Omega)} - |u - u_j|^2_{H^1(\Omega)} = C^2 2^{2s(1-j)} - C^2 2^{-2sj} = (1 - 2^{-2s}) C^2 2^{2s(1-j)}. \end{aligned}$$

This leads to $|u_j - u_{j-1}|_{H^1(\Omega)} = \sqrt{1-2^{-2s}}C2^{s(1-j)}$. Hence,

$$\log_2\left(\frac{|u_j - u_{j-1}|_{H^1(\Omega)}}{|u_{j+1} - u_j|_{H^1(\Omega)}}\right) = s.$$

In the same manner, one can show that if

$$2^{sj}|u - u_j|_{H^1(\Omega)} \to C \quad \text{as } j \text{ increases},$$

then

$$\log_2\left(\frac{|u_j - u_{j-1}|_{H^1(\Omega)}}{|u_{j+1} - u_j|_{H^1(\Omega)}}\right) \to s \quad \text{as } j \text{ increases}.$$

Acknowledgements

The first author was supported in part by the NSF Grant DMS-1418853, by the Natural Science Foundation of China (NSFC) Grant 11628104, and by the Wayne State University Grants Plus Program.

References

[1] T. Apel. *Anisotropic finite elements: local estimates and applications.* Advances in Numerical Mathematics. B. G. Teubner, Stuttgart, 1999.

[2] T. Apel and B. Heinrich. Mesh refinement and windowing near edges for some elliptic problem. *SIAM J. Numer. Anal.*, 31(3):695–708, 1994.

[3] T. Apel, A. L. Lombardi, and M. Winkler. Anisotropic mesh refinement in polyhedral domains: error estimates with data in $L^2(\Omega)$. *ESAIM Math. Model. Numer. Anal.*, 48(4):1117–1145, 2014.

[4] T. Apel and S. Nicaise. The finite element method with anisotropic mesh grading for elliptic problems in domains with corners and edges. *Math. Methods Appl. Sci.*, 21:519–549, 1998.

[5] T. Apel, A.-M. Sändig, and J. Whiteman. Graded mesh refinement and error estimates for finite element solutions of elliptic boundary value problems in non-smooth domains. *Math. Methods Appl. Sci.*, 19(1):63–85, 1996.

[6] T. Apel and J. Schöberl. Multigrid methods for anisotropic edge refinement. *SIAM J. Numer. Anal.*, 40(5):1993–2006 (electronic), 2002.

[7] I. Babuška and A. K. Aziz. On the angle condition in the finite element method. *SIAM J. Numer. Anal.*, 13(2):214–226, 1976.

[8] C. Bacuta, H. Li, and V. Nistor. Anisotropic graded meshes and quasi-optimal rates of convergence for the FEM on polyhedral domains in 3D. In *CCOMAS 2012 - European Congress on Computational Methods in Applied Sciences and Engineering*, e-Book Full Papers, pages 9003–9014. 2012.

[9] C. Bacuta, V. Nistor, and L. Zikatanov. Improving the rate of convergence of high-order finite elements on polyhedra. II. Mesh refinements and interpolation. *Numer. Funct. Anal. Optim.*, 28(7-8):775–824, 2007.

[10] A. Buffa, M. Costabel, and M. Dauge. Anisotropic regularity results for Laplace and Maxwell operators in a polyhedron. *C. R. Math. Acad. Sci. Paris*, 336(7):565–570, 2003.

[11] C. De Coster and S. Nicaise. Singular behavior of the solution of the Helmholtz equation in weighted L^p-Sobolev spaces. *Adv. Differential Equations*, 16(1-2):165–198, 2011.

[12] S. Brenner and L. Scott. *The mathematical theory of finite element methods*, volume 15 of *Texts in Applied Mathematics*. Springer-Verlag, New York, second edition, 2002.

[13] P. Ciarlet. *The Finite Element Method for Elliptic Problems*, volume 4 of *Studies in Mathematics and Its Applications*. North-Holland, Amsterdam, 1978.

[14] M. Costabel, M. Dauge, and S. Nicaise. Weighted analytic regularity in polyhedra. *Comput. Math. Appl.*, 67(4):807–817, 2014.

[15] M. Dauge. *Elliptic boundary value problems on corner domains*, volume 1341 of *Lecture Notes in Mathematics*. Springer–Verlag, Berlin, 1988.

[16] R. Fritzsch. *Optimale Finite-Elemente-Approximationen für Funktionen mit Singularitäten*. 1990. Thesis (Ph.D.)–TU Dresden.

[17] D. Gilbarg and N.S. Trudinger, *Elliptic partial differential equations of second order*. Springer-Verlag, 1977.

[18] P. Grisvard. *Elliptic Problems in Nonsmooth Domains*. Pitman, Boston–London–Melbourne, 1985.

[19] P. Grisvard. Edge behavior of the solution of an elliptic problem. *Math. Nachr.*, 132:281–299, 1987.

[20] V. Kondrat′ev. Boundary value problems for elliptic equations in domains with conical or angular points. *Trudy Moskov. Mat. Obšč.*, 16:209–292, 1967.

[21] V. A. Kozlov, V. G. Maz′ya, and J. Rossmann. *Elliptic boundary value problems in domains with point singularities*, volume 52 of *Mathematical Surveys and Monographs*. American Mathematical Society, Providence, RI, 1997.

[22] M. Křížek. On the maximum angle condition for linear tetrahedral elements. *SIAM J. Numer. Anal.*, 29(2):513–520, 1992.

[23] H. Li. An anisotropic finite element method on polyhedral domains: interpolation error analysis. *Math. Comp.*, DOI: https://doi.org/10.1090/mcom/3290.

[24] J.-L. Lions and E. Magenes. *Non-homogeneous boundary value problems and applications. Vol. I*. Springer-Verlag, New York, 1972. Translated from the French by P. Kenneth, Die Grundlehren der mathematischen Wissenschaften, Band 181.

[25] D. Schötzau, C. Schwab, and T. P. Wihler. *hp*-dGFEM for second-order mixed elliptic problems in polyhedra. *Math. Comp.*, 85(299):1051–1083, 2016.